https://doi.org/10.5194/egusphere-2024-949
Preprint. Discussion started: 13 May 2024
© Author(s) 2024. CC BY 4.0 License.

Risk of compound flooding substantially increases in the future Mekong River delta

Melissa Wood[1], Ivan D. Haigh[1], Quan Quan Le[2], Hung Nghia Nguyen[2], Hoang Tran Ba[2], Stephen E. Darby[3], Robert Marsh[1], Nikolaos Skliris[1], Joël J.-M. Hirschi[4]

[1] School of Ocean and Earth Science, University of Southampton, Waterfront Campus, European Way, Southampton, SO14 3ZH, UK
[2] Southern Institute of Water Resources Research (SIWRR), 658th Vo Van Kiet Avenue, Ward 1, District 5, Ho Chi Minh city, Vietnam
[3] School of Geography and Environmental Science, University of Southampton, Highfield, Southampton, UK
[4] National Oceanography Centre Southampton, European Way, Southampton, SO14 3ZH, UK

Correspondence to: Ivan Haigh (I.D.Haigh @soton.ac.uk)

Abstract

Floods are consistently identified as the most serious global natural hazard, causing devastating loss of life and economic damages that run into multiple billions of dollars each year. At the coastline, many flood disasters are in fact compound flood events, with two or more flood drivers occurring concurrently or in quick succession. In coastal regions the combined effect of fluvial (river) and coastal (storm-tides – storm surges plus high astronomical tides) floods together has a greater impact than if each occurred separately. Deltas in south-east Asia are particularly exposed to coastal compound floods as they are low-lying, densely populated regions subject to both intense rainfall and tropical cyclone (TC) derived storm tides. For our study we used a sophisticated 1D river model, combined with 2D storm tide levels, to analyse past/present and future compound flood hazard and exposure for the Mekong River delta, one of the most flood-vulnerable deltas in the world. We found that with compound flooding a greater area of the delta will be inundated, some parts will flood to greater flood depth. Central areas around Ang Giang and the Dong Thap provinces would be particularly impacted. In the future delta, the impact of compound flooding is potentially more significant, as compound floods inundate a greater area, to greater depth in many locations, and floods last longer too. Compound flooding therefore has clear implications for flood managers of the future delta, who will need to ensure that existing and future flood defences are to the right standard and in the right locations to offer effective protection against this future risk.

1 Introduction

The United Nations Office for Disaster Risk Reduction estimates that, between 2010 and 2019, a total of 1.65 billion people have been affected by flood events worldwide, with 104,614 deaths (UNDRR, 2020). A relatively large proportion of these deaths and losses have occurred in low-lying coastal regions, particularly in deltas. Water related disasters are a major issue in deltas because, located at the nexus of the marine environment and major rivers, the land is exposed to flooding from both. Globally around 339 million people live on deltas– that is approximately 4.5% of the population living on just 0.57% of the Earth's land surface area (Edmonds et al., 2020). Some global deltas are 'drowning' due to combinations of land subsidence (from groundwater extraction or the decline of fluvial sediment loads), sea-level rise, and changes in storminess associated with climate change (Brown and Nicholls, 2015). This exacerbates flood risk, and it tends to be poorer delta inhabitants that are most

https://doi.org/10.5194/egusphere-2024-949
Preprint. Discussion started: 13 May 2024
© Author(s) 2024. CC BY 4.0 License.

vulnerable to its consequences. Their livelihoods are more likely to depend directly on the delta, their homes and assets are less protected, they are less financially resilient, and they are more prone to health impacts (Hallegate et al., 2016).

Flooding in deltas can be greatly exacerbated when two or more flood sources occur concurrently, or in close succession, resulting in disproportionately extreme events referred to as 'compound flooding' (Kew et al., 2013; Wahl et al., 2015; Ward 2018; Couasnon et al., 2020; Camus et al., 2021). The Intergovernmental Panel on Climate Change (IPCC) defines compound events as: (1) two or more extreme events occurring simultaneously or successively, (2) combinations of extreme events with underlying conditions that amplify the impact of the events, or (3) combinations of events that are not themselves extremes but lead to an extreme event when combined (Seneviratne et al., 2012). Zscheischler et al. (2018) describes compound flooding as 'the combination of multiple drivers and/or hazards that contributes to societal or environmental risk'.

Tropical, and sub-tropical, cyclones and storms deliver prime conditions for compound flooding - depositing large volumes of rainfall, and driving storm surges at the coast from strong winds and lowered air pressure. A number of destructive historic floods around deltas are now considered to have been compound events. When Super Typhoon Hato made landfall around Macao and Hong Kong on 23 August 2017, the intense rainfall, winds, astronomical tides and storm surges all combined to flood urban coastlines of the Pearl River Delta Estuary, China by up to 1.29 m. This affected 2.46 million people, with thirty two people declared dead or missing (Wang et al 2019). Just two days later, Hurricane Harvey landed in in Houston, Texas, USA. Intense rainfall over four days led to record rain depths over a wide area with the hurricane forcing a storm-tide of between 2.40 m and 3.05 m (8-10 ft) above Mean Higher High Water level at the coast (Chambers et al., 2018; Blake and Zelinsky 2018). Seventy people died in this complex flood that defied the standard classification - half the fatalities occurred beyond the Federal Emergency Management Agency's (FEMA's) designated 1:500-year flood zone extents (Sebastian et al., 2017; Jonkman et al., 2018; Wahl et al., 2018; Valle-Levinson et al., 2020).

Despite the growing evidence, until relatively recently, few studies focused on compound flood hazard in large river deltas (Collins et al., 2019; Green et al., 2024). In delta environments, flood studies tended to assume a constant mean sea level boundary, leading to an underestimation of flood depths. However, Eilander et al. (2020), created a global river model bounded by dynamic sea level conditions with storm surges, and found that compound effects influenced flood levels at the majority of coastal locations, for high probability events. Eilander et al., (2023) subsequently coupled a high-resolution 2D hydrodynamic Super-Fast INundation of CoastS (SFINCS) model, with CaMa-Flood (Yamazaki et al., 2013; Hirabayashi et al., 2021) and the Global Tide and Surge Model (GTSM) (Muis et al., 2020) to examine compound effects from pluvial, fluvial, and tropical cyclone (TC) induced storm surge drivers at Mozambique's coastline. Again confirming that interactions between flood drivers will amplify total water levels. Around the same time, Bates et al. (2021) modelled the interactions between fluvial, pluvial, and coastal flood hazards, for the coastline of the conterminous USA, finding that there would be some significant local changes from the expected flood envelope because of compound flooding interactions.

https://doi.org/10.5194/egusphere-2024-949
Preprint. Discussion started: 13 May 2024
© Author(s) 2024. CC BY 4.0 License.

Statistical dependence analysis has also been used in a range of global/regional scale studies to assess the likelihood of different extreme drivers occurring at similar times (e.g., Zheng et al., 2013; Wahl et al., 2015; Bevacqua et al., 2019). Prior studies have shown that statistical dependence between flood drivers means extreme combinations are more likely. Ignoring such dependency can lead to underestimation of return periods at the river mouth (Ward et al., 2018; Couasnon et al., 2020; Camus et al., 2021). The research warns that future coastal flooding due to mean sea level rise can be aggravated by compound interactions. They found that dependence can variably influence the joint probability of river discharge and storm surge extremes, having important implications for our understanding of flood statistics and probability along impacted coastlines.

Current research points to populations living along Asian and African deltas and coastlines being most exposed to future coastal flooding, due to atmospheric climate changes driving tropical and sub-tropical storm surge events in these regions (Seto 2011; Neumann et al., 2015). Consequently, the aim of this paper is to characterise the past/present and future compound flood risk, from TC induced extreme river discharges and storm-tides, to one of the most flood-vulnerable and populated deltas in southeast Asia: the Mekong River delta in Vietnam. The Mekong River delta is located in a region of intense TC activity: the Western North Pacific. Storm tides driven by TC events are a tangible hazard for many low lying coastal communities in this region, on top of relative sea-level rise (Vousdoukas et al., 2016; Calafat et al. 2022; Wood et al., 2023). Mean sea levels (MSLs) in the South China Sea surrounding the delta rose by 3.5 mm/year at Vung Tau, Vietnam between 1985-2010 (Hak et al., 2016). While TCs currently impact the Red River Delta in north Vietnam more frequently, TCs do strike south Vietnam and the Mekong River delta also. In 1997, Tropical Storm Linda killed 3,111 people across the Mekong River delta, destroyed 300,000 homes, and flooded 4,500 km^2 of rice paddy crop (Dun, 2011; Anh et al., 2017). In December 2017, 650,000 people were evacuated from vulnerable areas of Southern Vietnam including the Mekong River delta, because of Typhoon Tembin. Climate change is likely to increase the flood risk to Vietnam in the coming decades. In 2019 the IPCC identified the future Mekong River delta as being at risk not only from sea-level rise and soil erosion, but also from high tides and cyclones (Oppenheimer et al., 2019). The region is projected to experience increased storminess which would lead to more intense rainfall events as well as extreme sea levels from TC induced storm surges (Dasgupta et al. 2007; Seneviratne et al. 2012; Hirabayashi et al., 2013; Tessler et al., 2015; Lin and Emanuel, 2016; IPCC 2021; Skliris et al.,2022; Wood et al., 2023).

In pursuit of our aim, this paper has three objectives: (1) to examine how compound flood hazard differs across the delta compared to flood hazard driven by river-only or storm-tide-only events under past/present day conditions; (2) to explore how compound flooding will change over time due to projected climate change; (3) and to assess which regions of the delta are river, coastal, or compound-flood dominated, and how this might change over time with climate change. We achieve these objectives by using an existing MIKE 11 hydrodynamic model of this area and apply new river discharge and storm-tide boundary conditions. We simulate a range of combined flooding scenarios, with differing return periods of river discharge at the upstream boundary and storm-tide at and downstream, and compare those flood-extents and durations against the single-source flood results. We contrast river discharges and storm-tides that reflect a past/present climate and a future climate. We then use a compound ratio approach on the model outputs to quantify which regions of the delta are river, coastal or compound flood dominated.

https://doi.org/10.5194/egusphere-2024-949
Preprint. Discussion started: 13 May 2024
© Author(s) 2024. CC BY 4.0 License.

The structure of the paper is therefore as follows. The Mekong River delta study region is described in Section 2. The model set up is discussed in Section 3, with model scenarios and simulations described in Section 4. Results are presented in Section 5, with key findings and discussion in Section 6. Conclusions are given in Section 7.

2 Study location

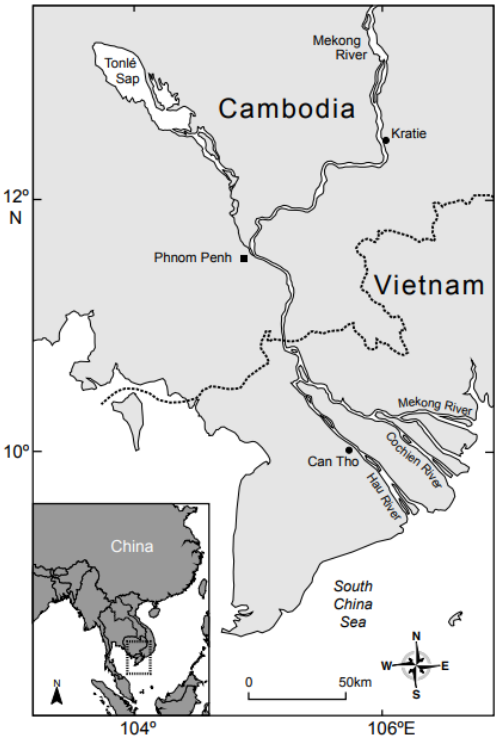

Figure 1 Location of the Mekong River

The Mekong River delta (Fig. 1) is home to ~20% of Vietnam's ~98.5 million 2021 population, with around a quarter of this population living within 2 m of current MSL (Edmonds 2020; Nguyen 2021; GSO, 2024). The delta's importance for jobs and food security cannot be understated. It produces up to 50% of the nation's rice, 65% of aquaculture, and 70% of its fruit (Dun, 2011; Van et al., 2012; Triet et al., 2020).

The region owes its fertile land to regular flooding, following seasonal rainfall. The local climate supports two monsoon systems which together generate around 85% of annual river flows in the Mekong River, over the wet season (May to November) (Nguyen 2021). Wet season floods can have two flood peaks. A principal 'good' flood always arrives between July and early September as a response to monsoonal rainfall (Dung 2011; Nguyen 2021). A second peak can sometimes be observed between September and October, and is linked to rain from tropical depressions, storms and cyclones from the South China Sea making landfall over the ~795,000 km^2 Mekong River watershed (Hung et al., 2011). These can be so damaging they have been coined 'bad' floods, because they arrive unexpectedly, and can have higher peaks, or sustain flooding for longer at higher water levels, overwhelming local flood defences (Nguyen, 2021).

Farmers and local government started to intensively manage flood water levels in the late 1990s by heavily engineering the delta via miles of protective canals, pumps, gates, dykes, and sea walls (Hung et al., 2011; Welch et al., 2017; Nguyen 2021). Low dykes with crest levels at around 2.5 m (1.5 m to 4.0 m) above MSL are used to manage the annual flood peak and thereby extend the rice paddy season. These are also known as 'August dykes' to match the seasonal high water level (Wesselink et al., 2015; Thanh et al., 2020; Triet et al., 2020; Nguyen 2021). High dykes, with crest level approximately 4.0-6.0 m above MSL were introduced more recently in response to a series of extreme (bad) river floods (Thanh et al., 2020; Nguyen 2021). These function to cut off the

https://doi.org/10.5194/egusphere-2024-949
Preprint. Discussion started: 13 May 2024
© Author(s) 2024. CC BY 4.0 License.

floodplain from the natural flood inundation regime of the river, facilitating a third rice crop in select areas (Triet et al., 2020). Unfortunately, the engineered systems restrict natural deposition around the delta mouth, reducing delta stability and disrupting processes that protect the delta coastline from sea surges and high tides, compromising the long-term climate resilience of the delta (Käkönen et al., 2008; Welch et al., 2017; Day et al., 2016; Tessler et al., 2015).

3 Model set up

We used a Danish Hydraulic Institute's (DHI) MIKE 11 hydrodynamic model of the lower Mekong River and its delta. The model setup and domain are described in Section 3.1, a summary of the model channels, structures, boundary conditions and run parameters is given in Section 3.2 and the model calibration and validation is discussed in Section 3.3.

3.1 MIKE 11 model and domain

In this study we use a MIKE 11 hydrodynamic model of the Mekong River delta first developed in 2007 by the Vietnamese Southern Institute of Water Resources Research (SIWRR; Dung et al., 2011; Hung et al., 2012; Manh et al., 2014). The MIKE 11 model generates discharges within its network using an implicit, finite difference solution of the 1-dimensional shallow water (Saint Venant) equations. A fully 1-D approach is recommended for the lower Mekong River delta due to its size, its dense and heavily engineered network of rivers, canals, and pipes, and because of unique hydraulic processes occurring due to the river's connection with the Tônlé Sap Lake in Cambodia (Dung et al., 2011).

The model domain, channel network, cross sections and boundary locations are illustrated in Fig. 2a. The associated Mekong River delta Digital Elevation Model in Fig. 2b highlights the low lying nature of the lower delta, with median elevations around ~0.5m above MSL. It spans an area of ~55,000 km^2, ranging between 8°N and 14°N Latitude and 102°E and 107°E Longitude which encompasses its two distinctly different hydraulic regimes: the northern Cambodian Flood Plain (CFP) and the southern Vietnamese Mekong Delta (VMD). The upstream extents of the model are between Kratie and the Tônlé Sap Lake in Cambodia, and the downstream extents coincide with the coastal boundaries of the South China Sea and Gulf of Thailand in the VMD (Fig. 2a). The model was created in the WGS 1984 UTM Zone 48N coordinate system and has a local 'Hon Dau' vertical datum (Hoa et al., 2014) equivalent to local MSL. Elevations in the MIKE 11 model faithfully reproduce levels of between ~25 m above MSL around Kratie, ~12 m around the Tônlé Sap Lake, down to 0.3-0.7 m above MSL at the Vietnam coastline (Tri 2012).

https://doi.org/10.5194/egusphere-2024-949
Preprint. Discussion started: 13 May 2024
© Author(s) 2024. CC BY 4.0 License.

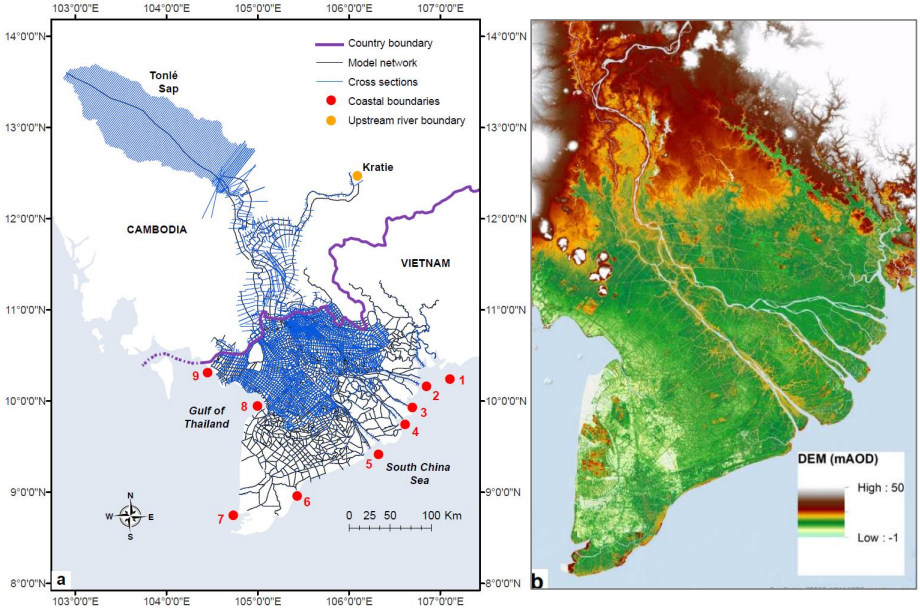

Figure 2 A: The MIKE 11 1-D Model network (black) with cross sections (blue) and coastal boundary locations (red). The 9 downstream boundaries are 1. Vũng Tàu, 2.Vàm kênh, 3. Bình Đại, 4. An Thuận, 5. Bến Trai, 6. Tran De, 7. Gành Hào, 8. Sông Đốc, 9.Rạch Giá / Xẻo Rô. B: A DEM illustrates the flat landscape of the Mekong River delta (GLO-30/FABDEM DEM)

While 1-D models can be appropriate for representing conveyance of water volumes in a well-defined channel, they don't always adequately represent more complex inundation in the floodplain, such as wetting and drying processes, or backflow (Bates et al, 2005; Ikeuchi et al., 2015, 2017). To address this the MIKE 11 model incorporates long and closely packed cross sections (i.e., 2-dimensional profiles created from ground survey data) in the wide natural floodplains of the Mekong River in the upper delta within Cambodia and around the Tônlé Sap Lake (Fig. 2a). Contrast this with the short cross sections (with attached storage cells) in the lower delta to represent the canalised channels fenced by dykes and adjoined by traditional terraced paddies within Vietnam.

Importantly, SIWRR recently updated the MIKE 11 model in three ways to improve performance. First, model dyke elevation data throughout the delta were updated from surveys undertaken between 2015 and 2018. Second, much of the model's channel bathymetry data were updated, from survey work undertaken by SIWRR and the University of Hull (described in Vasilopoulos et al., 2021). In that work, the most recent river discharge and stage data, measured at five internal gauge stations, were used to update channel roughness parameters throughout the model (Vasilopoulos et al., 2021; Le et al., 2022). Third, data from floodplain elevation surveys around Dong Thap province, carried out by SIWRR in 2019, have been incorporated.

https://doi.org/10.5194/egusphere-2024-949
Preprint. Discussion started: 13 May 2024
© Author(s) 2024. CC BY 4.0 License.

3.2 Model hydrology, structures, and parameters

The model is forced at the upstream boundary, by a single river discharge timeseries at Kratie, Cambodia (Fig. 2a). There are three main routes of floodwater entry into the Vietnamese Mekong Delta: (i) via the two main river channels the Mekong and Bassac in Cambodia (locally named as the Tien and Hau rivers, respectively, within Vietnam); (ii) via transboundary overland discharge via the Plain of Reeds located east of the Mekong River, and (iii) overland discharge to the west of the Bassac River (Fig. 1; Nguyen 2021). And the flows at Kratie feed all three of these routes of floodwater entry into the delta. Further details of the Kratie discharge timeseries, forcing the model, are given within Section 4.1. Minor inflows at the Border Plain and the eastern boundary vary between 0.8 m^3s^{-1} (fixed) and 953 m^3s^{-1} (varying with peak in September), but have a negligible impact on model results, hence we kept them constant for this study.

At the downstream limits of the model there are 58 coastal boundaries at points located around the Vietnam coastline (Fig. 2a). These are driven by storm-tides (e.g., astronomical tide plus storm surge) time-series in our model. These storm-tide boundary condition time series are described in more detail within Section 4.2.

An important hydraulic feature in the model is the Tônlé Sap Lake (the Great Lake) which acts as a reservoir storage area at the top of the model (Fig. 2a). As Mekong River discharges gradually rise during the monsoonal wet season, the Tônlé Sap Lake, and Cambodian floodplains, provides vital flood water storage and attenuation of the 'good' annual flood peak, for the lower delta. The Tônlé Sap Lake receives rainfall- (i.e., surface-) runoff inputs at a number of locations around its perimeter in the model, but has a single major inflow from the Mekong River near Phnom Penh to the south which only begins to spill over into the lake when river levels exceed ~17 m above MSL (Hoi 2005, equivalent to ~2.3m water depth: Le et al., 2022) at the start of the wet season. There is no evaporation from the lake in the model. At the end of the flood season, spillover from the Mekong River ceases, and the Tônlé Sap Lake starts to draw down again releasing floodwaters back into the Mekong River delta system (Nguyen 2021).

Table 1 – Overview of the Mekong River delta hydrodynamic model, modified from Dung et al., (2011)

Item	Count
Number of real branches	1,232
Length of simulated channel system	~20,860 km
Number of 'artificial' branches	2,170
Number of downstream boundary conditions	58
Number of upstream boundary conditions	3
Number of flood plain compartments	542

A key advantage of 1-D models is that discharge over hydraulic structures and supercritical/subcritical discharges is stably represented (DHI 2017), which is particularly important considering there are a large number of such structures within the Mekong River delta. The SIWRR MIKE 11 model that we used here includes measurements from a total of 542 flood-cell compartments enclosed by dykes and control structures (Table 1). In the model, dyke heights range between 0.8 and 6.5 m above MSL datum. There are also a total of 23 weirs and 2,260 sluice and gate structures for irrigation and flood level management. Sluice gates within the Vietnamese Mekong River

https://doi.org/10.5194/egusphere-2024-949
Preprint. Discussion started: 13 May 2024
© Author(s) 2024. CC BY 4.0 License.

delta are used to manage saline intrusion and flood levels within the protected areas, diverting flows to neighbouring and downstream compartments (Triet et al., 2020).

The model categorises rivers, channels, and floodplain into 5 separate classes according to their size and function. Channel roughness (resistance) defaults are defined according to these classes as detailed within Dung et al. (2011), using Manning's coefficient value, and summarised in Table 2. However, these default roughness values have also recently been fine-tuned (as described above, Vasilopoulos et al., 2021). Floodplain roughness is given a global Manning's value of 0.1.

Table 2 - Assignment of roughness values to five classes of channels and floodplains (copied from Dung et al., 2011)

No	Group's Name	Stricker's [Manning's] coefficient range		Description
		Min	Max	
1	MK_BS	20 [0.016]	60 [0.050]	Branches used to model the Mekong River in Cambodia, Bassac River and the Tônlé Sap Lake
2	TienHau	20 [0.016]	60 [0.050]	Tien River in Vietnam (Mekong River), Hau River in Vietnam (Bassac River), and major branches of these rivers
3	CamFP	10 [0.020]	50 [0.100]	Branches for modelling Cambodia floodplains
4	VietFP	10 [0.020]	50 [0.100]	Artificial branches for modelling Vietnam floodplains
5	Global	20 [0.016]	60 [0.050]	Other from above (remaining branches)

3.3 Model calibration and validation

For highly distributed numerical models to accurately replicate observed flood extents and levels, the model needs to be calibrated and validated against a wide range of discharge conditions, which can be a challenge if measured data is of poor quality or insufficiently spatially dispersed around the domain (Horritt and Bates, 2002). Fortunately, there is an abundance of data on the Mekong River delta that can be used. Dung et al., (2011) and Manh et al., (2014) used a mixture of time-series of ENVISAT earth observation satellite data products, and hydrometric data from a network of gauge stations to auto-calibrate, and validate, the model for high discharge events encompassing the floods of 2008, 2009 and 2011. These calibration exercises confirmed that the model is optimised for higher discharges and the annual flood – but would be further improved if dyke heights in the model could be better represented. Consequently, surveys of dykes, channel dimensions and floodplain were undertaken between 2015 and 2019 and this data incorporated in the model (Section 3.1).

In 2019 SIWRR carried out a further validation exercise to test the MIKE 11 model's suitability to characterise flood conditions in the Mekong River delta. SIWRR compared the river discharge and water level data at 5 (main) and 8 (medium) channel gauge stations internal to the model domain and independent of boundary data. The main river gauge stations were located at Can Tho, Chau Doc, My Thuan (now renamed Tran De), Vam Nao, and Tan Chau (as described in Vasilopoulos et al., 2021 and Le et al., 2022). Nash Sutcliffe efficiency coefficients were calculated, by finding the error between modelled and measured data at these locations for the year 2018. This gave a mean overall rating of 0.89 for river discharge (0.87 in dry season months January to May, and 0.91 in flood season months June to December), and a mean rating of 0.94 for river water levels (0.95 in dry season months, and 0.95 in flood season months). Any value above 0.8 is considered to show good model accuracy, so

https://doi.org/10.5194/egusphere-2024-949
Preprint. Discussion started: 13 May 2024
© Author(s) 2024. CC BY 4.0 License.

results again clearly demonstrated that the model can effectively simulate the higher discharges and water levels (e.g., Ritter and Muñoz-Carpena, 2013; Moriasi et al., 2007). Because of SIWRR's thorough and consistent work to calibrate and validate this MIKE 11 model for high flows, we did not implement any additional model validation.

4 Modelling approach

In this paper we assess potential compound flood hazard, from extreme river discharges and TC induced storm-tides, across the Mekong River delta, using a number of representative scenarios. For both river and storm-tide, we created seven scenarios: a baseline flood event, a 10% (1 in 10 year), a 2% (1 in 50 year), a 1% (1 in 100 year), a 0.4% (1 in 250 year), a 0.2% (1 in 500 year), and a 0.1% (1 in 1000 year) Annual Exceedance Probability (AEP) flood event. We do not assess the precise likelihood of these events, as measured datasets are currently too short to derive accurate dependence statistics between drivers. All possible combinations of coastal and river compound flooding are then simulated. We run simulations for a wet season in the past/present (year 2020 - representative of the period 1980-2017), and a wet season in the future (year 2050 - representative of the period 2015-2050), including climate change.

We begin with a description of the creation of upstream river conditions in Section 4.1, and downstream coastal boundary condition creation in Section 4.2. The different compound flood combinations and the scenarios contrasting past/present, and future, compound floods are described in Section 4.3. Finally, in Section 4.4 we describe how the model simulation results were post-processed for analysis.

4.1 River boundary condition

We used a four-step process to create design return period scenario discharges for Kratie, Cambodia as the upstream boundary condition to the MIKE 11 model. Step one, we create a baseflow hydrograph for Kratie flows, encompassing the full wet season with a peak in late August/early September, with 10 minute time steps. This was achieved by taking the median of all (January 1924 to December 2013) daily flow data at Kratie, obtained from the Mekong River Commission (www.mrcmekong.org). A long timeseries baseflow hydrograph is important to model accuracy, as antecedent conditions in the wider delta strongly influences how extreme flood waters are distributed and what flood storage is physically available. This baseflow is illustrated in Fig. 3a as a greyed-out area and represents our 'baseline' conditions scenario.

In step two, we estimate design return period flood discharges at Kratie, for TC-rainfall forced flood events. We did by using annual (block) maxima from the 1924-2013 daily flow record, and assigning a rank (m) to the maxima from each year, from largest to smallest. Since extreme discharges at Kratie all occur under the same wet-season climate conditions, and annual maxima peaks are hydrologically independent of each other, then statistical conditions are met to apply the Gringorten formula and estimate river discharge probability of exceedance and return period values. The Gringorten formula was chosen due to its suitability for estimating extreme values and its demonstrable record for unbiased return period estimation (Guo, 1990). The probability of exceedance (P) using this formula is:

https://doi.org/10.5194/egusphere-2024-949
Preprint. Discussion started: 13 May 2024
© Author(s) 2024. CC BY 4.0 License.

$$P = \frac{(m-a)}{(n+2a)} \quad (1)$$

where *a* is a scale parameter equal to 0.44, and *n* is the number of annual maxima observations. The discharge return period at Kratie is given as 1/P. Our desired return period values are then interpolated, based on these data. The AEP is the percentage chance that a given discharge will be equalled or exceeded in any given year, based on these years of data. We therefore estimated 'design' return period discharge values for the 0.1% , 0.2%, 0.4%, 1%, 2% and 10% AEP levels.

In step three, we create a flood event pulse shape using an approach described in Yue et al., (2002). This method identifies typical flood event variables - event mean and event variance - from river gauge measurements, and creates a two-parameter beta probability density function (pdf) to produce a synthetic flood pulse shape of appropriate height (peak discharge) and width (duration). We isolated extreme flood event mean and variance values in the 1924-2013 Kratie discharge record to thus create a synthetic flood pulse shape characteristic of historic flood pulses at Kratie. We scaled the height to represent the appropriate discharge rate required for each of our design return period flood event scenarios (step two, Table 3). Lastly, we compared the flood duration and total flood volume contained in this synthetic flood pulse, with historic events, to confirm that it also carries a credible volume of flood water into the past/present delta.

Table 3 Peak discharge (m^3s^{-1}) for the 10% (1 in 10 year), 2% (1 in 50 year), 1% (1 in 100 year), 0.4% (1 in 250 year), 0.2% (1 in 500 year) and 0.1% (1 in 1,000 year) AEP floods at Kratie, Cambodia. For present (by 2020) and future (by 2050) climates.

	Annual Exceedance Probability (%)					
	10	**2**	**1**	**0.4**	**0.2**	**0.1**
Present	62,682	69,501	71,780	74,312	75,920	77,303
Future	71,067	78,869	81,420	84,215	85,963	87,448

Finally, in step four, we attempt to align the time to peak, between the river and storm surge flood surges, so they coincide and compound within the model. Through an iterative process of model simulations, we determined that the optimal time to have the peak occur upstream at Kratie, was 3.3 days before any storm tide strikes at our chosen section of Vietnam coastline. This would generate a river discharge flood peak which combines, with the storm-tide, around the centre of the delta; near to Can Tho on the Hau (Bassac) River/Vinh Long on the Tien (Mekong) River.

https://doi.org/10.5194/egusphere-2024-949
Preprint. Discussion started: 13 May 2024
© Author(s) 2024. CC BY 4.0 License.

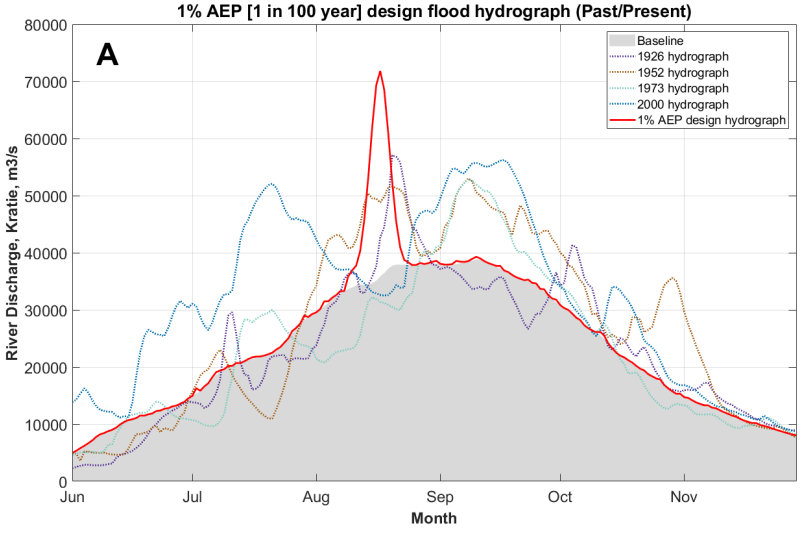

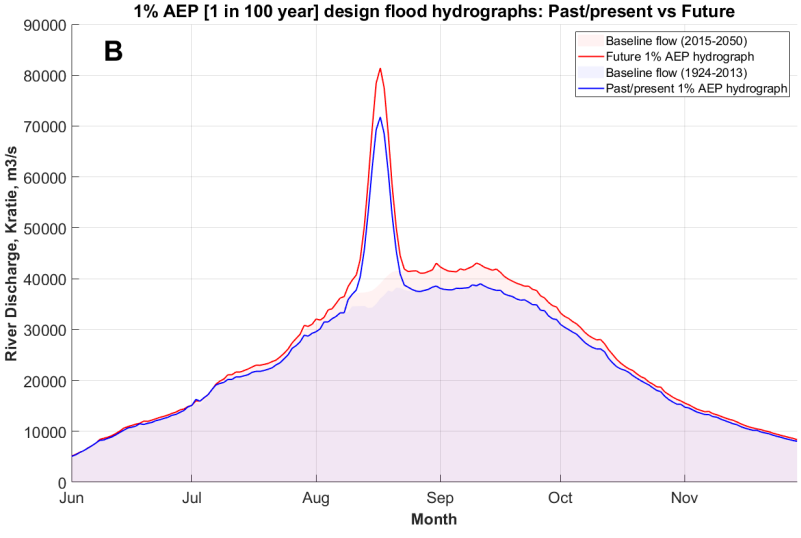

Figure 3 – (A) Red line: A past/present 1% AEP return period design flood hydrograph used as an upstream boundary condition in the model. This is combines a baseflow hydrograph (greyed-out area) with a single extreme flood event at the required date. Annual hydrographs for years 1926, 1952, 1973 and 2000 are also shown for comparison (dashed coloured lines). (B) - The 1% AEP flood hydrograph at Kratie for year 2020 (blue) vs a 2050 future (red).

We created a future total flood hydrograph at Kratie, by following the same steps as for the past/present delta above. Future river discharges in the Mekong by 2050 are expected to be greater than today's flows, due to increased storminess and TC activity in the region from projected climate change. To represent these changes we utilised results from a HYPE (Hydrological Predictions for the Environment) hydrological model created for the past/present and future climate for the Mekong region (Du et al., 2020 and 2022). The future (up to the year 2050)

https://doi.org/10.5194/egusphere-2024-949
Preprint. Discussion started: 13 May 2024
© Author(s) 2024. CC BY 4.0 License.

HYPE model used HadGEM3-GC3.1 climate model input data with local CMIP-RCP8.5 rainfall projections (Skliris et al., 2022). They HYPE future model predicts more intense rain days, and a larger number of dry days for the future Mekong region. However due to the coarse resolution of the climate input data, discharge values at Kratie appear to be underestimated in both past/present and future HYPE model outputs, contrary to other projections for South Vietnam which predicts at least a 5% increase in river flows here (Västilä et al., 2010; Skliris et al., 2022; Try et al., 2022). HYPE future has mean discharge output at Kratie that is actually 3% less than past/present day gauged values. Du et al., (2022) confirms that some river discharges linked to uncertain precipitation can be underestimated in the HYPE model. Since the future HYPE model does regionally follow projected trends overall, we have assumed that the results for Kratie represent a localised anomaly.

Consequently, to create future discharges for our MIKE 11 model, we chose to disregard the specific Kratie model outputs, and instead incorporate the overall trend for the region by using the differences between the past/present HYPE model outputs and the future HYPE model outputs instead. The procedure we used is as follows. Firstly, we ordered the timeseries of HYPE model output discharges, at Kratie, and calculated percentiles to these flows, for both the past/present and future results. We then calculated the percentage difference (δ), at every percentile, between the past/present and future HYPE river discharges. Plotting this out we observed that δ was largest for extreme high/low discharges, and smallest around the mean. Secondly, we increased the δ 50th percentile so it was equal to the +5% expected within the wider literature for future river flows here, and applied the same adjustment to all other δ values, creating δ+. Thirdly, we similarly ordered our Kratie gauged record (1924-2013) and created a ranking of observed river discharges by percentile, and then applied δ+ to estimate future river discharges. This method therefore combines both the general trend information by percentile from HYPE, with expected increases in mean flows around Kratie from the wider literature, and applies it to the past/present discharge record at Kratie. Using this approach, future river discharges have mean flows that have been increased by 5% during the wet season. Wet season high (95th percentile) river flows have been increased by ~11% and the low (5th percentile) flow extremes decreased by ~1%. This is entirely consistent with a future Mekong climate which is projected to have more intense rain days, and a larger number of dry days (Västilä et al., 2010; Try et al., 2022; Skliris et al., 2022).

The subsequent steps to create future design flood hydrographs for the MIKE 11 model are then identical to the past/present-day method described above. The 1% AEP hydrographs for year 2020 vs year 2050, are compared in Fig. 3b. The estimated peak discharges for the past/present and future periods, under our return period scenarios, are listed in Table 3.

4.2 Coastal boundary conditions

The Mike11 model has 58 coastal boundary points, shown in Fig. 2. However, only 9 points have a significant influence on water levels in the delta; the other 49 points represent channels with negligible impact on the delta. We create a suite of design return period storm-tides (i.e., astronomical tides plus storm surges) at each of the 9 principal coastal boundary points, representing a storm-tide associated with a TC crossing the Mekong River delta, using outputs from a prior study by Wood et al., (2023), for the same past/present and future years.

https://doi.org/10.5194/egusphere-2024-949
Preprint. Discussion started: 13 May 2024
© Author(s) 2024. CC BY 4.0 License.

We chose to model the storm surge striking one of the largest tributaries of the Mekong Delta coastline at the Co Chiên River mouth, near Thạnh Phong, Thạnh Phú District, Ben Tre, Vietnam (Point 4 on Fig. 2A). Wood et al. (2023) derived storm surge probabilities around the whole coastline of Vietnam, by driving a Mike21 coastal model with 10,000 years of synthetic TC activity from Bloemendaal et al., (2020, 2022), representative of a past/present (1980–2017) and high-emission-scenario future (2015–2050) period. We obtained storm surge information for the 10 largest past/present storms, at each of the 9 coastal boundary points, then calculated the average percentage scale factor as the storm surge reduces in size moving north or south of Point 4. We found that on average Points, 1, 2, 3 and 5, experience a surge that is 61%, 96%, 100% and 23% of the peak storm surge at Point 4. Point 6 experience a surge that is -45% of the peak surge at Point 4; this is because the wind direction is typically offshore from the track of the cyclone, generating a negative surge. At points 7, 8 and 9 the storm surge is on average negligible, and so we set this as 0% of the storm-tide height at Point 4. The resulting storm-tide boundary conditions are shown in Fig. 4.

We follow four steps to calculate storm-tide levels for the coastal boundaries of the model. First, we predict the astronomical tide for the duration of the model simulation using the T-Tide software package (Pawlowicz et al, 2002) in MATLAB, for June to November, at each of our 9 points (Fig. 2A). These are shown by the red line in Fig. 4, for each point. Second, we derive a design storm surge profile shape which has a length of ~2 days (±1 day around the peak), from the time-series of synthetic storm surges generated from the 10 largest events at Point 4, from Wood et al., (2023). We set the time and date of the storm surge peak to 07:30 20th August, to coincide with high water of a spring tide, and around the time of maximum river discharge (Section 4.1). The storm surge is shown by the magenta line in Fig. 4. Third, we scale the storm surge profile so that when combined with the astronomical tide, the peak storm tide corresponds with either the 0.1%, 0.2%, 0.4%, 1%, 2% or 10% design AEP level at this location. At the neighbouring 8 locations, we scale the storm surge profile by the percentage factor described above, to represent the decrease in strength of the storm surge further away from Point 4. Finally we combine design storm surge and astronomical tides. The blue line in Fig. 4 shows the combined storm-tide corresponding to the 1% AEP. Note, for the remainder of the simulation period, not shown in Fig. 4, the storm surge is set to zero. In this way, we create coastal boundary data files containing the full timeseries for all 9 coastal point locations, for each of the six AEPs and for of the past/present and future period. These coastal boundary sea level files have a timestep of 10 minutes.

https://doi.org/10.5194/egusphere-2024-949
Preprint. Discussion started: 13 May 2024
© Author(s) 2024. CC BY 4.0 License.

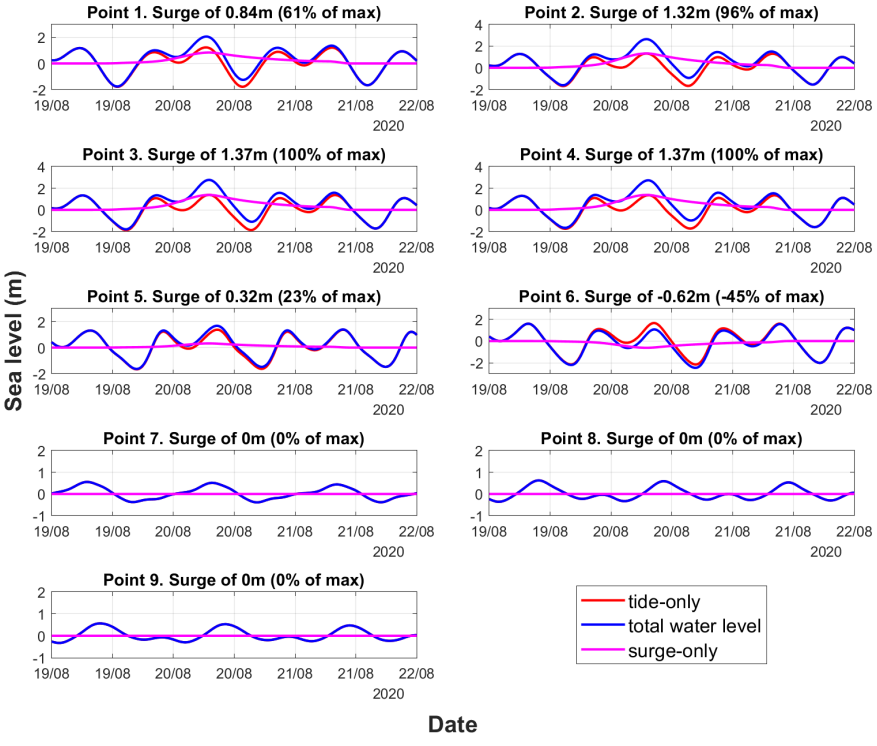

Figure 4 - The 1% AEP storm tide for each coastal boundary condition in the past/present climate is shown in blue. Red indicates the astronomical tide, and magenta shows the storm surge.

For the future period, we followed the same procedure but scaled the storm-tide to match the future AEP probabilities, also derived in Wood et al. (2023). The past/present and future storm-tide AEP are listed in Table 4, for Point 4. By the year 2050, the IPCC's 6th Assessment Report projects a relative MSL mean rise at the grid point adjacent to the Mekong River delta of 0.25 m, under the SSP5-8.5 reference scenario, relative to a 1995-2014 baseline (Fox-Kemper et al., 2021; NASA sea-level tool: https://sealevel.nasa.gov/ipcc-ar6-sea-level-projection-tool). The projected future storm tide heights we use in the model therefore have an additional 0.25 m added to capture this, as shown in brackets in Table 4.

Table 4 past/present (by 2020) and future (by 2050) storm tide heights (m) for the 10% (1 in 10 year), 2% (1 in 50 year), 1% (1 in 100 year), 0.4% (1 in 250 year), 0.2% (1 in 500 year) and 0.1% (1 in 1,000 year) AEP for Point 4. Values in square brackets are storm tide plus a projected future sea-level rise of 0.25 m.

	Annual Exceedance Probability (%)					
	10	**2**	**1**	**0.4**	**0.2**	**0.1**
Present	0.57	0.95	1.37	1.73	1.99	2.20
Future	0.53 [0.78]	1.55 [1.80]	1.89 [2.14]	2.34 [2.59]	2.57 [2.82]	2.66 [2.91]

https://doi.org/10.5194/egusphere-2024-949
Preprint. Discussion started: 13 May 2024
© Author(s) 2024. CC BY 4.0 License.

4.3 Model scenarios

We run 98 simulations of the model: 49 representing a past/present period, and 49 representing a future period. The past/present period is representative of TC activity derived from observations for the years 1980–2017 (Bloemendaal et al., 2021, 2022). The future period is representative of TC activity for the years 2015–2050 derived from high-resolution climate models driven with a high-emissions (SSP5-8.5) climate change scenario (Bloemendaal et al., 2022), and with a sea-level rise increase up to 2050 under the same SSP5-8.5 scenario from the IPCC 6th Assessment Report (Fox-Kemper et al., 2021).

We aim to determine the extent, influence, and duration of the full range of possible compound flood event combinations. Table 5 conveys the 49 combinations of river and coastal boundary conditions modelled in each time period. The baseline conditions for river discharge equal median daily flows at Kratie, and at the 9 coastal boundary points the coastal baseline conditions correspond to just astronomical tides (no storm surge). We timed our model boundary conditions to produce a state where Mekong River discharge and storm-tide combine to flood the central delta, coinciding around Can Tho on the Hau (Bassac) River and Vinh Long on the Tien (Mekong) River soon after the TC makes landfall.

Each of the 98 simulations in the MIKE 11 model were run from the 1st of June to 28th November. We used an adaptive timestep (minimum 1 minute, maximum 30 minutes), and selected the unsteady state option for river discharges as downstream sea levels, and upstream river discharges, volumes and velocities will all vary over time. We set an 'initial water level' value of between 0.5 m and 7.65 m in the major channels (1.5 m globally otherwise) at timestep zero. Also, a condition of no groundwater infiltration and no evaporation was set within the model, and a flood-calibrated default courant number was used (see Section 3.3). We set the simulation outputs to be a 3-hourly record of water level and discharge at all river channel output locations.

Table 5 Model combinations to synthesize a compound flood with river discharge flooding and storm tide flooding at the same time. The dark shaded boxes indicate results we reproduce as maps in this paper.

River discharge AEP (%), at Kratie	Storm-tide AEP (%), at coastal boundary Point 4						
	Tide-only	**10**	**2**	**1**	**0.4**	**0.2**	**0.1**
Baseline	✓	✓	✓	✓	✓	✓	✓
10	✓	✓	✓	✓	✓	✓	✓
2	✓	✓	✓	✓	✓	✓	✓
1	✓	✓	✓	✓	✓	✓	✓
0.4	✓	✓	✓	✓	✓	✓	✓
0.2	✓	✓	✓	✓	✓	✓	✓
0.1	✓	✓	✓	✓	✓	✓	✓

4.4 Presentation of model results

We present model results in four ways, showing variation relative to a flood baseline, with: (1) spatial flood difference maps; (2) profile plots along the Tien- Co Chiên River length, between Kratie and the Co Chiên river mouth; (3) flood depth hazard maps showing days of flooding at dangerous depths; and (4) spatial maps showing relative dominance of flood drivers.

https://doi.org/10.5194/egusphere-2024-949
Preprint. Discussion started: 13 May 2024
© Author(s) 2024. CC BY 4.0 License.

Spatial maps of flood extent for all scenarios in Table 5 were created by (i) using Environmental Systems Research Institute's (ESRI) ArcMap software to interpolate model maximum water elevations, at each river channel, outward using an inverse distance weighted tool. The interpolation and extension were confined to appropriate sub-basin limits (outlines obtained from https://data.opendevelopmentmekong.net). This flood layer was then (ii) applied to a high-resolution Digital Elevation Model (DEM) of the Mekong Delta. We used the FABDEM, based on the European Space Agency's Copernicus GLO-30 dataset (Hawker et al., 2022). The FABDEM vertical datum was reprojected to match the local Hon Dau model datum. Consequently, (iii) any flooding found below ground level were removed, as were floods over river channels and permanent bodies of water (e.g. Tônlé Sap Lake, areas of aquaculture). Finally, (iv) any islands of flood water not hydrologically connected to the coastline, or the river and canal network, were also removed using GIS tools. We repeated this process for every design flood scenario (Table 5), for both past/present and future scenarios. Hence, this process creates a series of spatially interpolated flood maps of the 1D model maximum water elevations, for the Mekong River delta. The final step was (v) to calculate flood *difference* maps by subtracting the past/present baseline flood map from the compound flood maps. Difference maps are created not only to highlight differences from the period baseline, but are also an attempt to remove systematic errors in the process of creating these flood maps.

Second, we examine the differences in flooding relative to a past/present baseline (i.e., median river discharges at Kratie, combined with only astronomical tide at all coastal boundaries), in profile view for all scenarios. We achieved this by extracting maximum flood elevations from the MIKE 11 model at points along the Mekong-Tien-Cochien River channel and plotted the additional depth of flooding, relative to our past/present baseline.

Third, we explore if there is a change in duration of dangerous flood levels, in compound scenarios over time (objective 2). We define a dangerous flood depth as a flood that is 0.5 m higher than our past/present baseline. This depth was selected because standing flood depths between ~0.5 m and ~1 m have been established to be unsafe for children, the elderly, and vehicles travelling through flooding (Smith, 2015). We did this by mapping the duration (number of days) and locations where flood depths exceed 0.5 m above our past/present baseline, creating 'flood depth hazard maps'.

Four, we present results showing which regions of the delta are river, coastal, or compound flood dominated (objective 3) in section 5.3. Our approach was to apply the 'compound ratio' method of Huang et al. (2021). For a given grid cell in our flood maps, the compound ratio (C_r) is the ratio between the maximum water level disturbance away from the baseline, and the sum of the two combined maximum disturbances, as follows:

$$C_r = \frac{\max(D)}{\sum_{j=1}^{2} \max(D_j)} \quad (2)$$

Disturbance (D) therefore is the height of maximum water level above the baseline state, as captured by our flood *difference* maps. C_r values close to 0 indicate substantial non-linear compound effects, while C_r values closer to 1 indicate negligible compound effects. To create compound ratio maps for this study, we applied the C_r equation on the flood difference maps, for different scenarios. The C_r maps in our results section are created in a two-step

https://doi.org/10.5194/egusphere-2024-949
Preprint. Discussion started: 13 May 2024
© Author(s) 2024. CC BY 4.0 License.

process. First, we took the flood difference map of a river flooding-only scenario (e.g. 1% AEP, with no storm tide component) for the numerator in Equation 2. The denominator is a difference map from a compound flood scenario with the same magnitude river flood (e.g. 1% AEP river flood with a 10% storm-tide flood). Every cell in the flood map will thus have a C_r value between 0 and 1, with values closer to 1 indicating river flooding dominance, and values closer to 0 indicating compound effects. This delivers the river portion of the C_r map. The process is then repeated for the storm tide parts of the C_r map. A storm-tide only difference map is used in the numerator to characterise storm-tide dominant flood areas in the domain. The denominator is a difference map from a compound flood scenario with the same magnitude storm-tide flood. Thereafter, the second step is to combine these two C_r maps, with the compound zones overlapping.

5 Results

The following sub-sections present our results as they relate to each of the three objectives outlined in section 1.

5.1 Differences between compound flood hazard and single-source flooding

We present areas of excess flood inundation for select past/present AEP scenarios (10%, 1% and 0.2%), relative to the past/present baseline, in Fig. 5Pa to 5Pp. In this matrix of figures, y-axis shows river flood magnitude scenarios, and x-axis shows storm-tide magnitude scenarios. To make allowance for margins of error, we present only flood differences greater than 0.1 m. Figure 5Pa - 5Pd, illustrate the increased area of coastal flooding around Point 4, linked to increasing magnitude of storm-tides. The excess flood depths ranges between ~0.25 m (10% AEP) and 3.0 m (0.2% AEP). The length of coastline impacted is around ~100 km. Inland this reaches approximately 160 km up the Mekong-Tien-Co Chiên river, up to around Cao Lanh in the 10% AEP storm-tide only flood (Fig. 5Pb) and up to Tan Chau at the Cambodia-Vietnam border in the 0.2% AEP flood (Fig. 5Pd). Whereas, for river-only flood scenarios (Fig. 5Pa, 5Pe, 5Pi, 5Pm), it is flood depths, rather than flood inundation area that changes with increasing flood magnitude. Floodwaters are largely confined to Cambodian and Tônlé Sap Lake areas, and northern parts of the Vietnam delta near the border. Between the Great Lake and the country border, north of Chau Doc in Vietnam, extra depth of flooding due to compound effects ranges between 0.3 m (10% AEP river flood) and 1 m (0.2% AEP river flood).

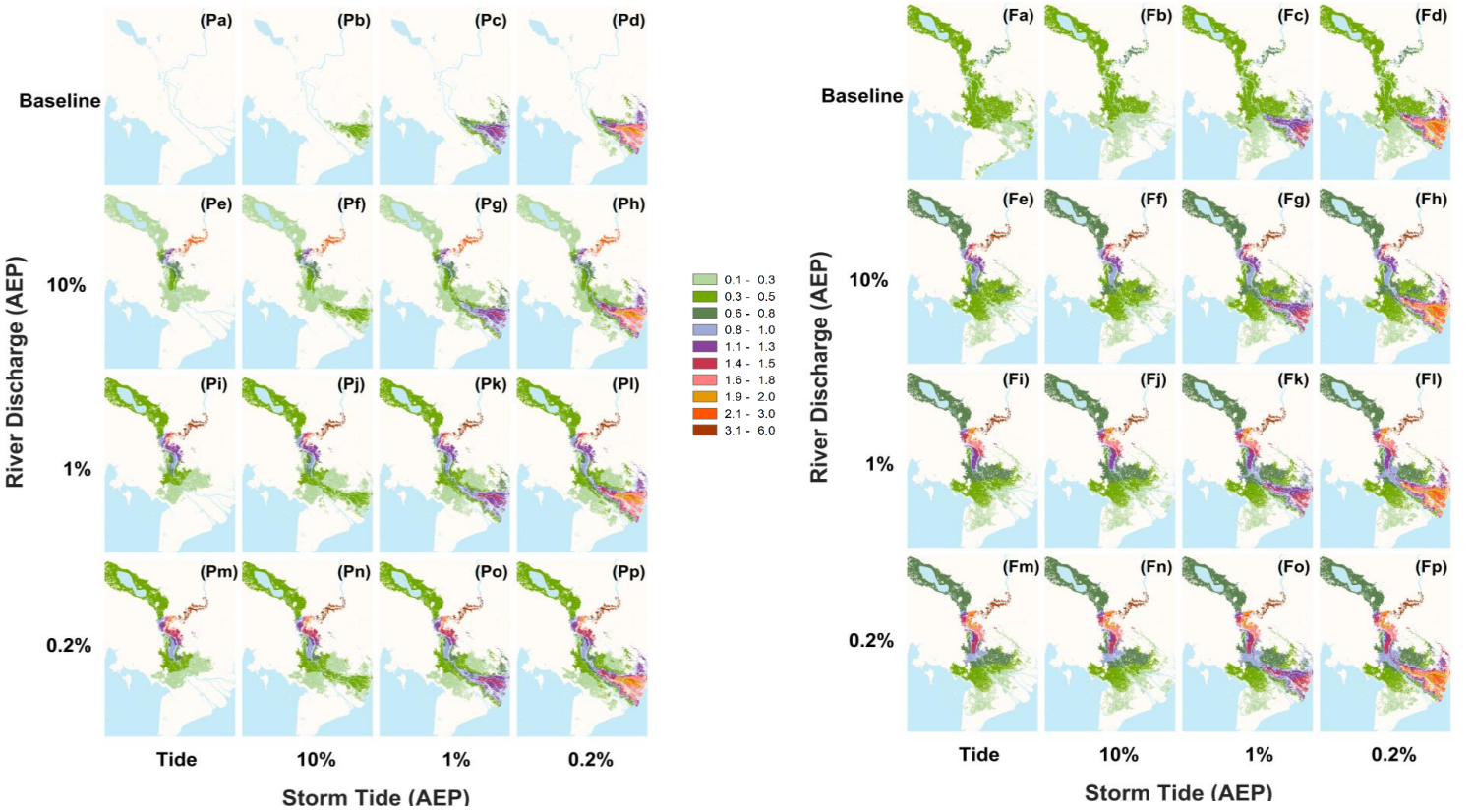

Figure 5 – Areas of excess flood inundation, greater than 0.1 m height, for various return period combinations. Depth difference ranges between 0.1 m and 6.0 m as shown in the legend (centre). On the left is 5Pa-5Pp: excess flooding in a past/present climate (up to year 2020), relative to the past/present baseline. On the right is 5Fa-5Fp: excess flooding in a future climate (up to year 2050), relative to the past/present baseline.

https://doi.org/10.5194/egusphere-2024-949
Preprint. Discussion started: 13 May 2024
© Author(s) 2024. CC BY 4.0 License.

https://doi.org/10.5194/egusphere-2024-949
Preprint. Discussion started: 13 May 2024
© Author(s) 2024. CC BY 4.0 License.

Compound river and storm-tide flooding appears to restrict how river discharges exit the network, resulting in up to an additional 0.5 m depth of flood water in the central compound zone, between the Bassac/Hau River near to Can Tho (Ang Giang province), and the Plain of Reeds around the Dong Thap province. This may be due to the delta structures and canal network being optimally designed to divert excess river flows to these neighbouring locations. But it is worth noting these areas do not normally experience spill-over in single-driver flood scenarios (Fig. 5Pe, 5Pi, 5Pm and Fig. 5Pb, 5Pc), unless the storm tide is very large (Fig. 5Pd). Further, the extent of storm tide progress inland varies when there is also a river flood. This is explored more in the long-section plot results described below. There is a ~70 km long stretch of river, between around Cao Lanh and Tan Chau, where compound flood hazard appears to present a particular danger, generating up to an additional ~1.5 m depth of flood water at the most extreme (≤1% AEP), in areas adjacent to the river (Fig. 5Ph, 5Pl, 5Pp). However, in general, the past/present flood difference maps appear to show that river and storm tide floods are largely distinct and separate within the delta, presumably a distinction that is modulated by the delta's engineered landscape. Where mixing does occur, excess flood depths increase and spill-over effects neighbouring areas.

Excess flood depths for the Mekong-Tien-Co Chiên River, relative to the past/present baseline, are shown in profile in Fig. 6a to 6d. In this profile plot the upstream extent is at Kratie (left) and downstream is the open sea (right). The top two panels show fixed coastal boundary conditions (a: no storm surge, b: 0.2% AEP storm-tide). The bottom two panels show fixed river flood conditions at Kratie (c: baseline river, d: 0.2% AEP river flood). Solid coloured lines indicate the past/present results. At the coastline, excess past/present flood depths reach ~0.25 m to ~1.8 m (10% to 0.2% AEP scenarios respectively), and this excess is maintained ~80 km inland along this stretch of river before it starts to decline. The past/present storm-tide dissipates around ~130 km (10% AEP) and ~175 km (0.2% AEP) inland. At the upstream end of this Mekong reach, excess river flooding appears extensive both in height (where the Mekong River channel narrows in Cambodia), and in extent (as it diverts into the Tônlé Sap Lake and descends into the delta, as seen in Fig. 5Pm). We see in Fig. 6a and 6d that large flood discharges can increase the normal annual river water level as far down the channel as 130 km from the coast. Consequently, there is a zone in the middle where river flooding and storm tide both influence flood levels, between ~130 km to ~180 km inland (between Sa Dec and Thanh Binh). When both river and storm-tide occur together, we see that the maximum heights of the storm-tide are somewhat pushed downstream towards the coastline. However, Fig. 6a and 6d together show that behind this, river flooding elevates flood levels in this same mixing region by ~ 0.2 m.

The area of excess flooding (in km^2), above baseline conditions is listed in Table 6, for each of the 49 past/present scenarios. A colour scale indicates the scenarios with the greatest difference in area away from the past/present baseline: green indicates small change, and red indicates a greater change in area. As expected, the areas of flood excess area increase with increasing flood magnitudes. The greatest flood area gains occur when the comparatively dry delta begins to fill with diverted river discharges. The system is of course designed to disperse these river flows efficiently, but gains in extent are added irregularly, symptomatic of a managed system. Sluice gates and weirs are designed to divert flows once a water level is reached. Zones flood as the storage becomes available, depending on topography.

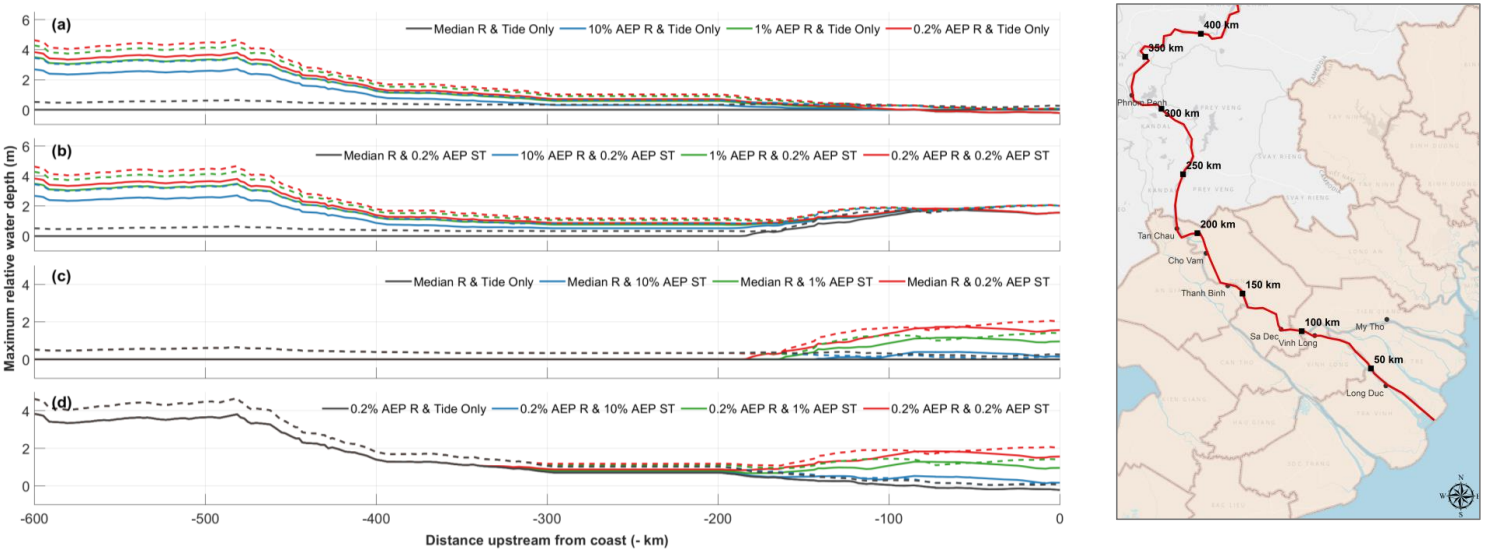

580 Figure 6 - Profile view of relative flood depth within the Mekong-Tien-Co Chiên River for past/present (solid line) and future (dashed line) climates. The future results include 0.25 m additional SLR at the coastline. Flood depths are relative to the past/present median river and tide-only simulation. The separate figures show (a) Median, 10%, 1% and 0.2% AEP return period river discharges vs tide-only (no surge); (b) Median, 10%, 1% and 0.2% AEP return period river discharges vs 0.2% AEP storm tide; (c) Fixed Median discharges in the river vs Median, 10%, 1% and 0.2% AEP return period storm tides; (d) Fixed 0.2% AEP return period river discharges vs Median, 10%, 1% and 0.2% AEP return period storm tides. Coastline is at the right side (0 km from coast) and Kratie is on the left (~600 km inland along this river line). Right figure: The Mekong-Tien-Co Chiên River line 0 km to 400 km from the coastline is shown in red.

https://doi.org/10.5194/egusphere-2024-949
Preprint. Discussion started: 13 May 2024
© Author(s) 2024. CC BY 4.0 License.

Table 6 - km^2 area of excess flooding above past/present baseline - for (a) past/present scenarios up to year 2020; and (b) future scenarios up to year 2050.

River Flood at Kratie (%AEP)		Storm-tide Flood (%AEP)													
		Past/Present (by year 2020) scenarios							Future (by year 2050) scenarios						
		Baseline	10	2	1	0.4	0.2	0.1	Baseline	10	2	1	0.4	0.2	0.1
	Baseline		4,687	6,370	7,377	8,362	9,385	10,035	28,185	29,202	33,743	33,950	34,358	34,587	34,713
	10	18,958	24,742	26,363	27,880	28,774	29,562	30,095	29,975	30,639	34,511	34,697	35,037	35,224	35,428
	2	21,084	26,741	28,636	29,811	30,559	31,223	31,576	30,221	30,863	34,614	34,796	35,130	35,342	35,543
	1	21,594	27,330	29,116	30,148	30,850	31,441	31,779	30,286	30,924	34,644	34,829	35,158	35,376	35,568
	0.4	22,524	28,414	29,583	30,466	31,153	31,692	32,003	30,379	31,008	34,690	34,870	35,202	35,418	35,603
	0.2	22,516	28,349	29,821	30,658	31,323	31,935	32,274	30,423	31,054	34,707	34,889	35,221	35,437	35,617
	0.1	23,156	28,745	30,189	30,953	31,596	32,097	32,409	30,487	31,103	34,735	34,912	35,244	35,467	35,634

Table 7 – Percentage increase in km^2 excess flood area between 2020 and 2050.

		Storm-tide Flood (%AEP)						
		Baseline	10	2	1	0.4	0.2	0.1
River Flood at Kratie (%AEP)	Baseline		523%	430%	360%	311%	269%	246%
	10	58%	24%	31%	24%	22%	19%	18%
	2	43%	15%	21%	17%	15%	13%	13%
	1	40%	13%	19%	16%	14%	13%	12%
	0.4	35%	9%	17%	14%	13%	12%	11%
	0.2	35%	10%	16%	14%	12%	11%	10%
	0.1	32%	8%	15%	13%	12%	10%	10%

590

https://doi.org/10.5194/egusphere-2024-949
Preprint. Discussion started: 13 May 2024
© Author(s) 2024. CC BY 4.0 License.

https://doi.org/10.5194/egusphere-2024-949
Preprint. Discussion started: 13 May 2024
© Author(s) 2024. CC BY 4.0 License.

Duration of flood inundation in the delta, beyond a past/present baseline, are shown in Fig. 7Pa to 7Pp for select AEP scenarios (10%, 1% and 0.2%). Again, the y-axis shows river flood magnitude scenarios, and the x-axis shows storm-tide magnitude scenarios. Blue and pink colours indicate days extra, up to 3 weeks. At the other extreme, flood duration of up to 2 months is given by brown and yellow colours. The past/present results show that it is river flooding in the Cambodian (upper) Mekong River delta that tends to flood for longer as magnitude of river flooding increases. The river flood hydrograph had duration of approximately 2 weeks (Fig. 3) in our simulation. In the canalised Vietnamese (lower) delta, flooding is distributed. Any direct or indirect (compound) flood impacts inland are contained to the channel or diverted, within short timescales (1-5 days). Flooding relating to storm-tide events at the coast only lasts ~2 days, as expect given the coastal boundary conditions (see Fig. 4).

5.2 Contrasting past/present and future compound flood risk

Building on our assessment of past/present compound flood characteristics in the delta, our second objective is to explore how compound flooding will change over time (up to 2050) due to a projected high-emission (SSP5-8.5) climate change scenario. Areas of excess flood inundation, relative to the past/present baseline, are shown in Fig. 5Fa to 5Fp, again for select AEP scenarios (10%, 1% and 0.2%). By 2050 we see a similar pattern to the past/present state in that river and storm-tide flooding are mostly separate processes within the delta. However, the impact of sea-level rise (0.25 m in this scenario) clearly impacts the subsequent excess depth of floodwaters during the storm-tide event. More of the lower delta (centred on Point 4) now has a substantial depth of extra flood water (1.5-2.0 m). The area covered by a 1% AEP storm-tide flood (river is baseline) in the past/present simulation is 7,377 km^2 and in the future simulation it is ~33,950 km^2 (a 4.6 times bigger area). Where in the past/present excess flood depths of ~1.5 m in the middle delta would only be projected during the most extreme 0.2% AEP storm surge (Fig. 5Pd, 5Ph, 5Pl, 5Pp); by 2050 this extra depth of flooding can be seen even during 1% AEP scenarios, and especially where river flooding occurs at the same time (Fig. 5Fg, 5Fk, 5Fo).

Similarly, future increased river discharges still flood the wider floodplains around the Tônlé Sap Lake and upper delta regions around the Cambodia-Vietnam border. In these wide and shallow floodplain areas, in all scenarios, the flood depth difference increases by ~0.25 m in the future (from around 0.1-0.5 m to around 0.3-0.8 m). In some locations future excess flood depths may reach 0.6-1.0 m for the first time, and these kind of depths may occur more often, as they are to be found in the more likely river flood event scenarios (the 10% AEP flood; Fig. 5Fe-Fp). Strangely, future storm-tides of 10% AEP (Fig. 5Fb, 5Ff, 5Fj, 5Fn) with SLR are not seen to flood the coastline to any substantial additional depth, relative to the past/present baseline.

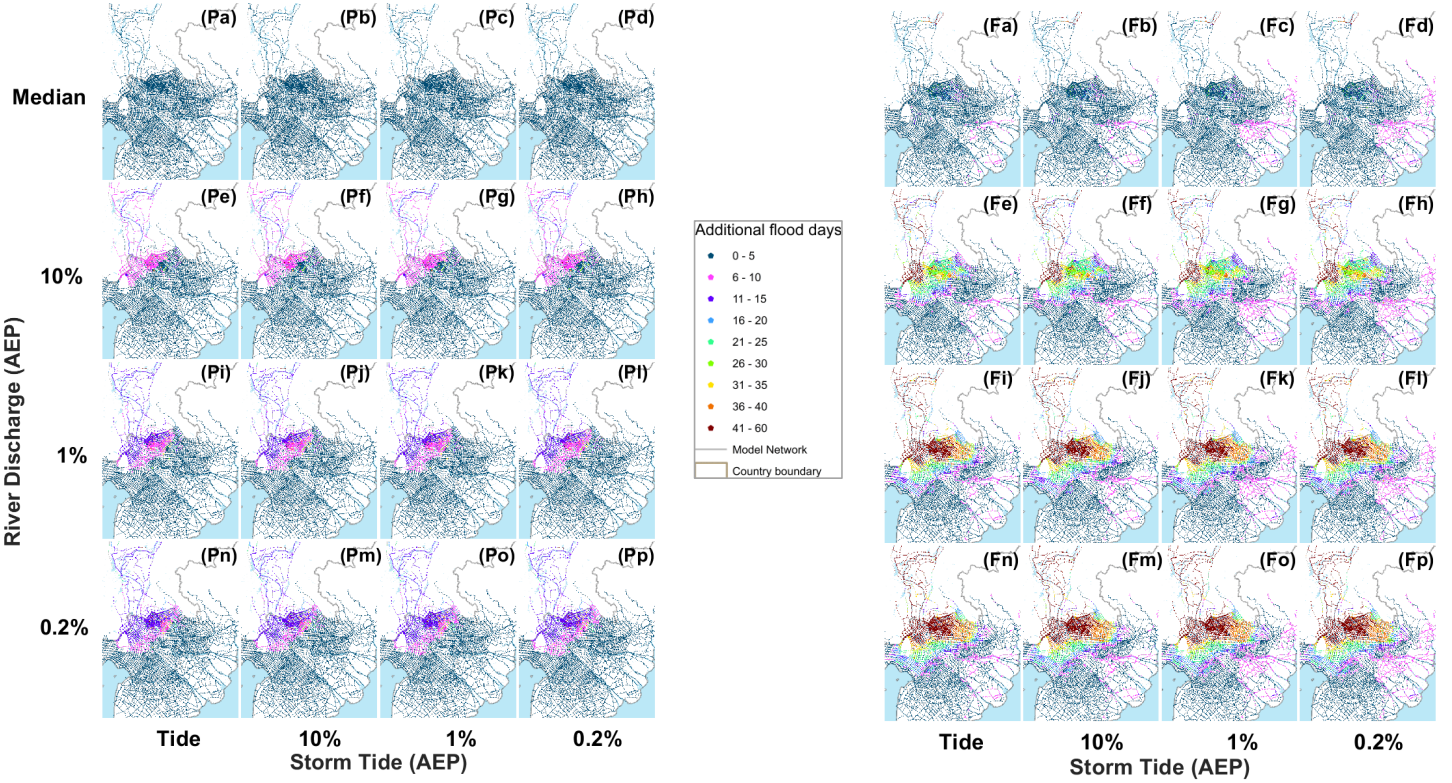

Figure 7 - Number of days that flood depths are over 0.5 m higher than the past/present baseline (Pa). Measured between 10 August and 29 September; for years 2020 (Pa-Pp) and 2050 (Fa-Fp).

https://doi.org/10.5194/egusphere-2024-949
Preprint. Discussion started: 13 May 2024
© Author(s) 2024. CC BY 4.0 License.

https://doi.org/10.5194/egusphere-2024-949
Preprint. Discussion started: 13 May 2024
© Author(s) 2024. CC BY 4.0 License.

The profile of excess future flooding, relative to the past/present baseline, is shown in Fig. 6 (dashed lines). At the coastline we see a sustained higher storm-tide excess flood height in larger magnitude storm-tides, that persists ~40 km further inland than we see today (Fig. 6d, 6e). At the upstream river boundary increases in future flows elevate flood levels by ~0.8m between Kratie station and the Cambodia/Vietnam border at -450 km inland. When there is compound flood (Fig. 6b, 6d), there is a ~70 km long stretch of river, between around Sa Dec and Tan Chau, where compound flood hazard appears to present a particular danger, at the most extreme generating up to an additional ~1.5 m depth of flood water in areas close to the Mekong-Tien-Co Chiên River channel (Fig. 5Ph, 5Pl, 5Pp).

The area of excess flooding (in km^2), for each of the 49 future scenarios, relative to the past/present baseline, is listed in Table 6. Table 7 shows the percentage increase in flood areas between the past/present and future scenarios. There is a marked increase in the excess flood area extent between the past/present and future scenarios. For example, around year 2050 the flood extent linked to a 10% AEP river flood, combined with a 1% AEP storm-tide, is around 24% bigger than the same event today. In the future scenarios, excess flood water is diverted towards parts of the lower delta previously unflooded. The south-west of the delta, around Hau Giang, Kien Giang and Bac Lieu provinces experiences up to an extra 0.5 m depth of flooding in the future. The area calculations in Table 6 also show that flooding will occur more frequently. For example, the additional flood area resulting from a combined low probability 0.4% AEP (1 in 250 year) storm tide with a 1% AEP (1 in 100 year) river flood in a past/present climate, is projected in the future to result from something like a more likely 10% AEP (1 in 10 year) river flood with a 2% AEP (1 in 50 year) storm tide.

Additional days of flood inundation in the future, relative to the past/present baseline, are shown in Fig. 7Fa to 7Fp. Results show that the major waterways of the lower delta around the coastline could, in the future, have up to 10 extra days of inundation due to the combination of SLR and storm-tide. But increasing storm-tide magnitude does not widen the coastal region affected. Flood waters are largely contained to the area east of the Bassac/Hau river, but there are a greater number of reaches which would transition from 0-5 days to 6-10 days as a result of such flooding (compare Fig. 7Po with Fig. 7Fo, for example). By contrast, the future Mekong delta is greatly affected by the increased river discharges in the upper delta zone around the Cambodia-Vietnam border. This area would have 0-15 days of additional flooding in only the median river flood scenario (Fig. 7Fa), due to increases in river flow as a result of climate change. This area today is the zone most likely to retain current floodwaters during a major flood in the Mekong delta. In the future 10% AEP scenario (all storm-tides) duration of flooding increases to 6 days to months extra, depending on the proximity to the main channel. Under the more extreme 0.2% AEP river flood, a large proportion of this area would be flooded for months longer than today.

5.3 Compound flood areas

Our third and final objective is to assess which regions of the delta are river, coastal, or compound flood dominated, and how this might change in the future with climate change. Maps of the Compound Ratio (Cr) are shown in Fig. 8 Pf to 8Pp (past/present), and Fig. 8Ff to 8Fp (future), for select (10%, 1% and 0.2% AEP combinations) return period scenarios. The red zones are river-dominant (i.e. have a Cr value of 0.8-1.0 when compared to a river-only flood scenario), blue zones are storm-tide-dominant (i.e. a Cr value of 0.8-1.0 when

https://doi.org/10.5194/egusphere-2024-949
Preprint. Discussion started: 13 May 2024
© Author(s) 2024. CC BY 4.0 License.

compared to a surge-tide-only flood scenario) and yellow areas indicate compound flooding regions (Cr value of 0-0.8).

Figure 8 highlights the tension between the two flood drivers during a compound flood event. Patently, river flooding is a major driver within the delta. The river dominant red zone is large in all scenarios, illustrating river dominance but also areas of natural flood storage and retention. As the magnitude of river flooding increases in the past/present delta (e.g. opposing a comparatively small 10% AEP magnitude storm-tide; Fig. 8Pf, 8Pj, 8Pn), flood extents barely grow due to the highly-engineered system for capture and redistribution. However if normal discharge routes into the sea become temporary inaccessible due to a larger storm-tide (Fig. 8Ph, 8Pl, 8Pp). This discharge turns inward spreading out into the lower delta and towards the Bassac River. This new flood extent is largely compound flood waters. The push and pull between the two flood drivers can also be seen with the movement of the compound zone: seawards as river dominant waters increase in magnitude (contrast Fig. 8Ph with Fig. 8Pn), and inland/upstream as storm surge become the dominant process (contrast Fig. 8Pf with Fig. 8Pp).

The same effects can be observed in the future results (Fig. 8F). However with greater flood volumes in the future, and projected higher storm-tides at the coast by year 2050, the compound zone is smaller, being squeezed with less apparent mixing. The areas of river or storm-tide dominance appear greater in the future too (e.g. contrast the red 1% AEP river flood, blue 1% AEP storm-tide floods of Fig. 8Pk with Fig. 8Fk). However there is also less apparent spillover into the central/Bassac River regions when a storm-tide blocks egress of river flood waters in the future. Of additional note is the model response to the future 10% AEP storm tide (Fig. 8Ff, 8Fj, 8Fn), where no blue zone storm-tide dominant waters are seen. Figure 5Pb (past/present) and Fig. 5Fb (future), together with the profile plots of Fig. 6c and 6d, tells us that the 10% AEP storm-tide is very close to baseline levels, particularly at the coastline. As such, the reason why this occurs could be that the settings of the past/present flood defences in the model effectively mitigate the 10% AEP flood in the future delta (i.e., flood gates are triggered early because climate change adds an additional 0.25 m to sea levels through the entire simulation), and/or the subtleties of the 10% AEP storm-tide are missed in our approach to mapping flood extents. More detailed modelling may be useful to clarify.

https://doi.org/10.5194/egusphere-2024-949
Preprint. Discussion started: 13 May 2024
© Author(s) 2024. CC BY 4.0 License.

Figure 8 Compound Ratio for the 10%, 1% and 0.2% combination of events, illustrating the relative dominance of river vs storm tide flood processes within the domain for past/present (left side: Pf-Pp) and future (right side: Ff-Fp) scenarios.

https://doi.org/10.5194/egusphere-2024-949
Preprint. Discussion started: 13 May 2024
© Author(s) 2024. CC BY 4.0 License.

6 Discussion

Results show that fluvial flooding in the Mekong River delta, coinciding with a storm-tide at the coast will bring the effects of compound flooding to central regions of the Vietnamese lower delta where the highly engineered network of dykes, flood gates, and weirs can efficiently divert flood waters above the 0.5 m (summer dykes) to ~4 m (winter dykes) thresholds, into compartments of rice paddies and fisheries, and redistribute the unwanted volumes into the sea. But because storm-tides act to oppose normal egress of high Mekong River flows around the struck coastline, compound flooding disrupts normal flood rerouting processes within some parts of the delta. Due to this temporary (~2-day) block, greater depth of flooding is observed upstream (1-6 m extra depth of flooding in the narrow channels between Kratie and Phnom Penh) in river dominant zones, and as much as an extra 3 m depth of flooding can occur in storm-tide dominant zones at the coastline (~100 km wide and, under 0.2% AEP flood conditions, up to ~160 km inland).

Should TC activity produce heavy rains regionally, and storm-tides to Vietnam's eastern coastline, the associated flood drivers at each end of the Mekong-Tien-Co Chiên River creates compound flooding in the main channel which spills into adjacent land: south-westwards around the Bassac/Hau River near to Can Tho (Ang Giang province), and north-eastwards towards the Plain of Reeds around the Dong Thap province. The compound zone extends along a ~50 km to ~80 km section of the upper and middle delta, up to the Cambodia-Vietnam border. The area covered varies with flood driver magnitude, in a scenario of 10% AEP river flooding combined with a 2% AEP storm surge would flood an extra ~26,300 km^2 of land above 0.1 m. Many Vietnam wards and communes in the central region will therefore experience new, or greater depths, of flooding relative to the 'good' flood welcomed by farmers annually. It is unknown how comprehensively potential compound flood risk from two or more drivers is considered within regional/local emergency and flood management plans. But compound flooding has clear consequences for inhabitants of these central areas, and thereafter for national food supply/security.

Results suggest that compound flooding in the future Mekong River delta will be of greater magnitude, last longer, and thus produce greater flood depths with more frequency than today. A greater area of the lower delta will be flooded overall, even for smaller magnitude compound events (a 1% AEP storm tide with a 1% AEP river flood scenario today is equivalent to a baseline flood by year 2050). Assuming that the population of Vietnam continues to grow, this indicates that by year 2050 more people will be impacted by compound flooding, more often. If more land area becomes inundated (even for low category storms), then flood managers in the Mekong River delta may have to consider flood resilience as standard for homes, infrastructure and future agriculture. If compound flooding is not deeply considered within future strategic plans for the Mekong River delta, a rethink may be needed. That rethink could focus on particular risks from compound flooding such as (i) overtopping of existing flood defences (river and sea dykes) and flood storage availability; (ii) the likelihood of compound flood inundation to new areas of the delta, currently not as well protected, and implications for its inhabitants; (iii) protecting high value land, and implications of future flooding on future land use needs; (iv) in a sinking delta what options are available to remove excess flood waters; (v) consideration of compound flood duration and the implications of this directly on local health (e.g. sanitation, drinking water), social welfare, livelihoods, transport

https://doi.org/10.5194/egusphere-2024-949
Preprint. Discussion started: 13 May 2024
© Author(s) 2024. CC BY 4.0 License.

and industrial systems; and finally (vi) the likely future demographics and what should be included within future (compound) flood evacuation plans.

7 Conclusions

The overall aim of this paper was to better understand the issue of compound river and storm-tide flooding in the Mekong River delta and how it changes over time, through the use of a detailed 1D MIKE 11 model, updated with recent survey data. Our results show that compound flooding is markedly different from single-driver flooding in the delta. In the present climate compound floods produce greater flood depths and flood into new areas of the delta (e.g. a modest 10% AEP river flood combined with a 2% AEP storm surge at the Mekong River mouth would flood an extra ~26,300 km^2 of land above 0.1 m). We identified an active compound zone within the central area of the Mekong River delta that is a mixture of storm-tide flooding and river flooding, and it changes shape and shifts depending on the magnitude of our two flood drivers.

In a future climate, sea level rise further exacerbates the compound hazard because a greater volume of water entering the delta will more quickly fills available flood storage areas, and storm tides begin at greater height. Our results suggest that, compared to today, future compound flooding increases in magnitude, duration and frequency in the Mekong River delta. A future delta with compound flooding that lasts longer in parts, and is likely to flood at higher levels, more often, has important implications for how the future delta is managed, and for the status of flood defences, standards and storage today. The complication of compound flooding is an important consideration for all deltas in Asian and African regions subject to a changing atmospheric climate over the coming decades. Any flood managers responsible for deltas in tropical and sub-tropical zones need to be aware of the extra hazards associated with TC-linked flooding today, and how this will change in the coming decades. Compound flooding will introduce extra considerations to not only flood defences, thresholds and flood detention/storage options, but also has implications for plans and policies relating to future land use, economic investment, population health, and access. Compound flooding may be best managed with layered defences over a wider area, with an eye to both future depth of flooding and future flood durations.

Future studies could explore the impact of this hazard where TCs make landfall at different locations/orientations, or of the impact of compound flooding in a delta with changing morphologies due to sand mining, coastal development, or land subsidence. In our analysis we employed a scenario assuming a worst case scenario of a TC strike and river flood peak occurring almost concurrently, at a date in the middle of the wet season. Variations of this set up will alter model outcomes and be interesting to explore.

https://doi.org/10.5194/egusphere-2024-949
Preprint. Discussion started: 13 May 2024
© Author(s) 2024. CC BY 4.0 License.

Data availability

Model results can be provided by the corresponding authors upon request.

Author contributions

IH, HNN, HTB, and SED planned the study and outline; QQL, NS, RM and JJMH supplied key information about/for the model, MW performed model simulations and analysed the data; MW and ID wrote the manuscript draft; QQL HNN, SD, RM, NS and JJMH reviewed and edited the manuscript.

Competing interests

The authors declare that they have no conflict of interest.

Acknowledgements

This work was supported by the UK Natural Environment Research Council (Grant Number NE/S003150/1), and the Ministry of Science and Technology of Vietnam and National Foundation of Science and Technology Development (NAFOSTED-RCUK fund). In personal communications, Dr Philip Minderhoud (Wageningen University) provided expert advice on the vertical datum adjustments required when working with local measurements in the Mekong River delta, and Dr Hal Voepel (University of Southampton) and Dr Christopher Hackney (Newcastle University) kindly shared processed river discharge data. The authors wish to acknowledge the use of the IRIDIS High Performance Computing facility, and associated support services at the University of Southampton in the completion of this work. We thank our Illustration Technician Kate Davis (University of Southampton), for creating key figures in this document. At the University of Bristol, we would like to thank Dr Laurence Hawker and Prof Jeff Neal for sharing FAB-Digital Elevation Model (FABDEM) data, of the Mekong River delta (https://data.bris.ac.uk/data/dataset/s5hqmjcdj8yo2ibzi9b4ew3sn). FABDEM is derived from the European Space Agency's Copernicus GLO 30 DEM data (https://copernicus-dem-30m.s3.amazonaws.com/readme.html). Lastly, we thank the German Aerospace Centre, DLR, for sharing TanDEM-X data of the Mekong Delta which was extremely useful to in our analysis (https://tandemx-science.dlr.de/ © DLR 2020).

https://doi.org/10.5194/egusphere-2024-949
Preprint. Discussion started: 13 May 2024
© Author(s) 2024. CC BY 4.0 License.

References

Arns, A., Wahl, T., Wolff, C., Vafeidis, A.T., Haigh, I.D., Woodworth, P., Niehüser, S. and Jensen, J., Non-linear interaction modulates global extreme sea levels, coastal flood exposure, and impacts. Nature communications, 11(1), p.1918. 2020.

Anh, L.T., Takagi, H., Thao, N.D. and Esteban, M., Investigation of awareness of typhoon and storm surge in the Mekong Delta–Recollection of 1997 Typhoon Linda. 土木学会論文集 B3 (海洋開発), 73(2), pp.I_168-I_173. 2017.

Anthony EJ, Brunier G, Besset M, Goichot M, Dussouillez P, Nguyen VL. Linking rapid erosion of the Mekong River delta to human activities. Scientific reports. Oct 8;5(1):1-2. 2015.

ADR. Australian Disaster Resilience Guideline 7-2: Technical Flood Risk Management Guideline: Flood emergency response classification of the floodplain, Australian Institute for Disaster Resilience CC BY-NC. 2014.

Bates, P.D., Quinn, N., Sampson, C., Smith, A., Wing, O., Sosa, J., Savage, J., Olcese, G., Neal, J., Schumann, G. and Giustarini, L.. Combined modeling of US fluvial, pluvial, and coastal flood hazard under current and future climates. Water Resources Research, 57(2), p.e2020WR028673. 2021.

Bates, P.D., Lane, S.N., and Ferguson R.I. Computational fluid dynamics modelling for environmental hydraulics." Computational fluid dynamics: applications in environmental hydraulics: 1-15. 2005.

Bevacqua, E., Maraun, D., Vousdoukas, M.I., Voukouvalas, E., Vrac, M., Mentaschi, L. and Widmann, M., Higher probability of compound flooding from precipitation and storm surge in Europe under anthropogenic climate change. Science advances, 5(9), p.eaaw5531. 2019.

Blake, E.S. and Zelinsky, D.A., National hurricane center tropical cyclone report: Hurricane Harvey (AL092017). National Hurricane Center: Silver Spring, MD, USA. 2018.

Bloemendaal, N., Haigh, I.D., de Moel, H., Muis, S., Haarsma, R.J. and Aerts, J.C., Generation of a global synthetic tropical cyclone hazard dataset using STORM. Scientific data, 7(1), p.40. 2020.

Bloemendaal, N., de Moel, H., Martinez, A.B., Muis, S., Haigh, I.D., van der Wiel, K., Haarsma, R.J., Ward, P.J., Roberts, M.J., Dullaart, J.C. and Aerts, J.C., A globally consistent local-scale assessment of future tropical cyclone risk. Science advances, 8(17), p.eabm8438. 2022.

Brown, S., Nicholls, R.J., Woodroffe, C.D., Hanson, S., Hinkel, J., Kebede, A.S., Neumann, B. and Vafeidis, A.T., Sea-level rise impacts and responses: a global perspective. Coastal hazards, pp.117-149. 2013.

Brown, S. and Nicholls, R.J., 2015. Subsidence and human influences in mega deltas: the case of the Ganges–Brahmaputra–Meghna. Science of the Total Environment, 527, pp.362-374

Brunner G.W., Savant G., and Heath R. E.; Modeler Application Guidance for Steady vs Unsteady, and 1D vs 2D vs 3D Hydraulic modelling. Hydrologic Engineering Center, Davis, California, USA. https://www.hec.usace.army.mil/publications/TrainingDocuments/TD-41.pdf. 2020

Camus, P., Haigh, I.D., Nasr, A.A., Wahl, T., Darby, S.E. and Nicholls, R.J., Regional analysis of multivariate compound coastal flooding potential around Europe and environs: sensitivity analysis and spatial patterns. Natural Hazards and Earth System Sciences, 21(7). 2021.

https://doi.org/10.5194/egusphere-2024-949
Preprint. Discussion started: 13 May 2024
© Author(s) 2024. CC BY 4.0 License.

Calafat, F.M., Wahl, T., Tadesse, M.G. and Sparrow, S.N.: Trends in Europe storm surge extremes match the rate of sea-level rise. Nature, 603(7903), pp.841-845. 2022.

Chambers, K.A., Husain, I., Chathampally, Y., Vierling, A., Cardenas-Turanzas, M., Cardenas, F., Sharma, K., Prater, S. and Rogg, J., Impact of Hurricane Harvey on healthcare utilization and emergency department operations. Western journal of emergency medicine, 21(3), p.586. 2020.

Chaumillon, E., Bertin, X., Fortunato, A.B., Bajo, M., Schneider, J.L., Dezileau, L., Walsh, J.P., Michelot, A., Chauveau, E., Créach, A. and Hénaff, A., Storm-induced marine flooding: Lessons from a multidisciplinary approach. Earth-Science Reviews, 165, pp.151-184. 2017.

Codiga, D.L., Unified Tidal Analysis and Prediction Using the UTide Matlab Functions. Technical Report 2011-01. Graduate School of Oceanography, University of Rhode Island, Narragansett, RI. 59pp. ftp://www.po.gso.uri.edu/pub/downloads/codiga/pubs/2011Codiga-UTide-Report.pdf. 2011.

Coleman JM, Huh OK, Braud D. Major world deltas: A perspective from space. Lousiana State University. 2003.

Collins M., M. Sutherland, L. Bouwer, S.-M. Cheong, T. Frölicher, H. Jacot Des Combes, M. Koll Roxy, I. Losada, K. McInnes, B. Ratter, E. Rivera-Arriaga, R.D. Susanto, D. Swingedouw, and L. Tibig, 2019: Extremes, Abrupt Changes and Managing Risk. In: IPCC Special Report on the Ocean and Cryosphere in a Changing Climate [H.-O. Pörtner, D.C. Roberts, V. Masson-Delmotte, P. Zhai, M. Tignor, E. Poloczanska, K. Mintenbeck, A. Alegría, M. Nicolai, A. Okem, J. Petzold, B. Rama, N.M. Weyer (eds.)]. 2019.

Couasnon, A., Eilander, D., Muis, S., Veldkamp, T. I. E., Haigh, I. D., Wahl, T., Winsemius, H. C., and Ward, P. J.: Measuring compound flood potential from river discharge and storm surge extremes at the global scale, Nat. Hazards Earth Syst. Sci., 20, 489–504, https://doi.org/10.5194/nhess-20-489-2020, 2020.

Dasgupta S, Laplante B, Meisner C, Wheeler D, Yan J.; The impact of sea level rise on developing countries: a comparative analysis. World Bank Policy Research Working Paper 4136, World Bank, Washington D.C. 2007.

Day, J.W., Agboola, J., Chen, Z., D'Elia, C., Forbes, D.L., Giosan, L., Kemp, P., Kuenzer, C., Lane, R.R., Ramachandran, R. and Syvitski, J., Approaches to defining deltaic sustainability in the 21st century. Estuarine, coastal and shelf science, 183, pp.275-291. 2016.

DHI, M., 1D-DHI Simulation Engine for 1D River and Urban Modelling-Reference Manual. 2017.

Du, T.L., Lee, H., Bui, D.D., Graham, L.P., Darby, S.D., Pechlivanidis, I.G., Leyland, J., Biswas, N.K., Choi, G., Batelaan, O. and Bui, T.T., Streamflow Prediction in Highly Regulated, Transboundary Watersheds Using Multi-Basin Modeling and Remote Sensing Imagery. *Water resources research*, *58*(3). 2022.

Du, T.L., Lee, H., Bui, D.D., Arheimer, B., Li, H.Y., Olsson, J., Darby, S.E., Sheffield, J., Kim, D. and Hwang, E., Streamflow prediction in "geopolitically ungauged" basins using satellite observations and regionalization at subcontinental scale. *Journal of Hydrology*, *588*, p.125016. 2020.

Dun, O., Migration and displacement triggered by floods in the Mekong Delta. International Migration, 49, pp.e200-e223. 2011.

Dung, N.V. and Thang, T.D., Establishment of a large scale hydrodynamic model for modelling floods in the Mekong Delta using MIKE11, SIWRR–Southern Institute of Water Resour. Res. Ho Chi Minh City. 2007.

https://doi.org/10.5194/egusphere-2024-949
Preprint. Discussion started: 13 May 2024
© Author(s) 2024. CC BY 4.0 License.

Dung, N.V., Merz, B., Bárdossy, A., Thang, T.D. and Apel, H., Multi-objective automatic calibration of hydrodynamic models utilizing inundation maps and gauge data. Hydrology and Earth System Sciences, 15(4), pp.1339-1354. 2011.

Edmonds, D.A., Caldwell, R.L., Brondizio, E.S. and Siani, S.M., Coastal flooding will disproportionately impact people on river deltas. Nature communications, 11(1), p.4741. 2020.

Eilander, D., Couasnon, A., Leijnse, T., Ikeuchi, H., Yamazaki, D., Muis, S., Dullaart, J., Winsemius, H.C. and Ward, P.J., A globally-applicable framework for compound flood hazard modeling. Nat. Hazards Earth Syst. Sci., 23, 823–846, https://doi.org/10.5194/nhess-23-823-2023. 2023.

Eilander, D., Couasnon, A., Ikeuchi, H., Muis, S., Yamazaki, D., Winsemius, H. C., & Ward, P. J. The effect of surge on riverine flood hazard and impact in deltas globally. Environmental Research Letters, 15(10), 1-12. [104007]. https://doi.org/10.1088/1748-9326/ab8ca6. 2020.

Emanuel, K., The great east Pakistan cyclone of November 1970. Divine wind: the history and science of hurricanes, pp.221-25. 2005.

Emanuel, K., Response of global tropical cyclone activity to increasing CO2: Results from downscaling CMIP6 models, Journal of Climate, 34(1), pp.57-70, 2021.

Eskander, S.M. and Barbier, E.B., Long-term impacts of the 1970 cyclone in Bangladesh. World Development, 152, p.105793. 2022.

Gray, W.M., Tropical cyclone genesis in the western North Pacific. Journal of the Meteorological Society of Japan. Ser. II, 55(5), pp.465-482. 1977.

Gray, W.M., Tropical cyclone genesis (Doctoral dissertation, Colorado State University. Libraries). 1975.

Green, J., Haigh, I., Quinn, N., Neal, J., Wahl, T., Wood, M., Eilander, D., de Ruiter, M., Ward, P. and Camus, P., A Comprehensive Review of Coastal Compound Flooding Literature. EGU24, (EGU24-1669). 2024.

GSO – General Statistics Office of Vietnam. https://www.gso.gov.vn/en/population. Accessed: 24 March 2024.

Haigh, I.D., Eliot, M. and Pattiaratchi, C.: Global influences of the 18.61 year nodal cycle and 8.85 year cycle of lunar perigee on high tidal levels. Journal of Geophysical Research: Oceans, 116(C6). 2011.

Hallegatte, S., Shock waves: managing the impacts of climate change on poverty. World Bank Publications. 2016

Hak, D., Nadaoka, K., Bernado, L.P., Le Phu, V., Quan, N.H., Toan, T.Q., Trung, N.H., Van Ni, D. and Van, P.D.T., Spatio-temporal variations of sea level around the Mekong Delta: their causes and consequences on the coastal environment. Hydrological Research Letters, 10(2), pp.60-66. 2016.

Harley, M., Coastal storm definition. Coastal storms: Processes and impacts, pp.1-21. 2017.

Haque, A., Haider, D., Rahman, M.S., Kabir, L. and Lejano, R.P., Building Resilience from the Grassroots: The Cyclone Preparedness Programme at 50. International journal of environmental research and public health, 19(21), p.14503. 2022.

Hawker, L., Uhe, P., Paulo, L., Sosa, J., Savage, J., Sampson, C. and Neal, J., A 30 m global map of elevation with forests and buildings removed. Environmental Research Letters, 17(2), p.024016. 2022.

Hoa, H.M., Construction of initial national quasi-geoid model VIGAC2017, first step to national spatial reference system in Vietnam. Vietnam Journal of Earth Sciences. 2017a, 39(2), pp.155-166. 2017.

https://doi.org/10.5194/egusphere-2024-949
Preprint. Discussion started: 13 May 2024
© Author(s) 2024. CC BY 4.0 License.

Hoi, T.N., Research on scientific and technological solutions on building dike system for sustainable development in the Mekong Delta, Southern Institute of Water Resour. Res., Ho Chi Minh City. 2005.

Hirabayashi, Y., Mahendran, R., Koirala, S., Konoshima, L., Yamazaki, D., Watanabe, S., Kim, H. and Kanae, S., Global flood risk under climate change. Nature climate change, 3(9), pp.816-821. 2013.

Horritt, M. S., and P. D. Bates. Evaluation of 1D and 2D numerical models for predicting river flood inundation. Journal of hydrology 268, no. 1-4: 87-99. 2002

Horsburgh, K.J. and Wilson, C., Tide-surge interaction and its role in the distribution of surge residuals in the North Sea. Journal of Geophysical Research: Oceans, 112(C8). 2007

Hossain, I. and Mullick, A.R., Cyclone and Bangladesh: A historical and environmental overview from 1582 to 2020. *International Medical Journal*, 25(6), pp.2595-2614. 2020.

Huang, W., Ye, F., Zhang, Y.J., Park, K., Du, J., Moghimi, S., Myers, E., Pe'eri, S., Calzada, J.R., Yu, H.C. and Nunez, K., Compounding factors for extreme flooding around Galveston Bay during Hurricane Harvey. Ocean Modelling, 158, p.101735. 2021.

Hung, N.N., Delgado, J.M., Tri, V.K., Hung, L.M., Merz, B., Bárdossy, A. and Apel, H., Floodplain hydrology of the Mekong delta, Vietnam. Hydrological Processes, 26(5), pp.674-686. 2012.

Idier, D., Bertin, X., Thompson, P., & Pickering, M. D.. Interactions between mean sea level, tide, surge, waves and flooding: mechanisms and contributions to sea level variations at the coast. Surveys in Geophysics, 40, 1603-1630. 2019.

Ikeuchi, H., Hirabayashi, Y., Yamazaki, D., Muis, S., Ward, P.J., Winsemius, H.C., Verlaan, M. and Kanae, S., Compound simulation of fluvial floods and storm surges in a global coupled river-coast flood model: Model development and its application to 2007 C yclone S idr in B angladesh. Journal of Advances in Modeling Earth Systems, 9(4), pp.1847-1862. 2017.

IPCC. Climate Change 2021: The Physical Science Basis. Contribution of Working Group I to the Sixth Assessment Report of the Intergovernmental Panel on Climate Change [Masson-Delmotte, V., P. Zhai, A. Pirani, S.L. Connors, C. Péan, S. Berger, N. Caud, Y. Chen, L. Goldfarb, M.I. Gomis, M. Huang, K. Leitzell, E. Lonnoy, J.B.R. Matthews, T.K. Maycock, T. Waterfield, O. Yelekçi, R. Yu, and B. Zhou (eds.)]. Cambridge University Press, Cambridge, United Kingdom and New York, NY, USA. 2021

Jonkman, S.N., Godfroy, M., Sebastian, A. and Kolen, B., Brief communication: Loss of life due to Hurricane Harvey. Natural Hazards and Earth System Sciences, 18(4), pp.1073-1078. 2018.

Le, T.V.H., Nguyen, H.N., Wolanski, E., Tran, T.C. and Haruyama, S., The combined impact on the flooding in Vietnam's Mekong River delta of local man-made structures, sea level rise, and dams upstream in the river catchment. Estuarine, Coastal and Shelf Science, 71(1-2), pp.110-116. 2007.

Le Quan, Q., Vasilopoulos, G., Hackney, C., Parsons, D., Nghia, H.N., Darby, S. and Houseago, R., Sediment routing though the apex of a mega-delta under future anthropogenic impacts and climate change (No. EGU22-9871). Copernicus Meetings. 2022.

Lee, W., Sun, A.Y. and Scanlon, B.R., 2024. Probabilistic Storm Surge and Flood-Inundation Modeling for the Texas Gulf Coast Using Super-Fast INundation of CoastS (SFINCS). Authorea Preprints.

Lin, N. and Emanuel, K., Grey swan tropical cyclones. Nature Climate Change, 6(1), pp.106-111. 2016.

https://doi.org/10.5194/egusphere-2024-949
Preprint. Discussion started: 13 May 2024
© Author(s) 2024. CC BY 4.0 License.

Luu, C., Von Meding, J. and Kanjanabootra, S., Analysing flood fatalities in Vietnam using national disaster database and tree-based methods. Natural Hazards and Earth System Sciences Discussions, pp.1-32. 2017.

Käkönen, Mira. "Mekong Delta at the Crossroads: More Control or Adaptation?" Ambio, vol. 37, no. 3, pp. 205–12. JSTOR. 2008.

Kew, S. F., Selten, F. M., Lenderink, G., and Hazeleger, W.: The simultaneous occurrence of surge and discharge extremes for the Rhine delta, Nat. Hazards Earth Syst. Sci., 13, 2017–2029, https://doi.org/10.5194/nhess-13-2017-2013. 2013.

Kirezci, E., Young, I.R., Ranasinghe, R., Muis, S., Nicholls, R.J., Lincke, D. and Hinkel, J., Projections of global-scale extreme sea levels and resulting episodic coastal flooding over the 21st Century. Scientific reports, 10(1), p.11629. 2020.

Manh, N.V., Dung, N.V., Hung, N.N., Merz, B. and Apel, H., Large-scale suspended sediment transport and sediment deposition in the Mekong Delta. Hydrology and Earth System Sciences, 18(8), pp.3033-3053. 2014.

McGranahan, G., Balk, D. and Anderson, B., The rising tide: assessing the risks of climate change and human settlements in low elevation coastal zones. Environment and urbanization, 19(1), pp.17-37. 2007.

Minderhoud, P.S.J., Erkens, G., Pham, V.H., Bui, V.T., Erban, L., Kooi, H. and Stouthamer, E., Impacts of 25 years of groundwater extraction on subsidence in the Mekong delta, Vietnam. Environmental research letters, 12(6), p.064006. 2017.

Moriasi, D.N., Arnold, J.G., Van Liew, M.W., Bingner, R.L., Harmel, R.D. and Veith, T.L.. Model evaluation guidelines for systematic quantification of accuracy in watershed simulations. Transactions of the ASABE, 50(3), pp.885-900. 2007.

Muis, S., Apecechea, M.I., Dullaart, J., de Lima Rego, J., Madsen, K.S., Su, J., Yan, K. and Verlaan, M., A high-resolution global dataset of extreme sea levels, tides, and storm surges, including future projections. Frontiers in Marine Science, 7, p.263. 2020.

Muis, S., Verlaan, M., Winsemius, H.C., Aerts, J.C. and Ward, P.J., A global reanalysis of storm surges and extreme sea levels. Nature communications, 7(1), p.11969. 2016.

MunichRe Flood risks on the rise: underestimated natural hazard, devasting damage. https://www.munichre.com/en/risks/natural-disasters-losses-are-trending-upwards/floods-and-flash-floods-underestimated-natural-hazards.html . 2021. Accessed: 27 February 2023.

Neumann, B., Vafeidis, A.T., Zimmermann, J. and Nicholls, R.J., Future coastal population growth and exposure to sea-level rise and coastal flooding-a global assessment. PloS one, 10(3), p.e0118571. 2015.

Nicholls, R.J., Lincke, D., Hinkel, J., Brown, S., Vafeidis, A.T., Meyssignac, B., Hanson, S.E., Merkens, J.L. and Fang, J., A global analysis of subsidence, relative sea-level change and coastal flood exposure. Nature Climate Change, 11(4), pp.338-342. 2021.

Nicholls, R.J. and Cazenave, A., Sea-level rise and its impact on coastal zones. Science, 328(5985), pp.1517-1520. 2010.

Nguyen, K.A., Liou, Y.A. and Terry, J.P., Vulnerability of Vietnam to typhoons: A spatial assessment based on hazards, exposure and adaptive capacity. Science of the Total Environment, 682, pp.31-46. 2019.

https://doi.org/10.5194/egusphere-2024-949
Preprint. Discussion started: 13 May 2024
© Author(s) 2024. CC BY 4.0 License.

Nguyen, V.K.T.; Flood dynamics in the Vietnamese Mekong Delta: Current state and future projections. Diss. Universität Potsdam Potsdam. https://publishup.uni-potsdam.de/opus4-ubp/frontdoor/deliver/index/docId/51283/file/nguyen_diss.pdf. 2021

Oppenheimer, M., B.C. Glavovic, J. Hinkel, R. van de Wal, A.K. Magnan, A. Abd-Elgawad, R. Cai, M. Cifuentes-Jara, R.M. DeConto, T. Ghosh, J. Hay, F. Isla, B. Marzeion, B. Meyssignac, and Z. Sebesvari: Sea Level Rise and Implications for Low-Lying Islands, Coasts and Communities. In: IPCC Special Report on the Ocean and Cryosphere in a Changing Climate [H.-O. Pörtner, D.C. Roberts, V. Masson-Delmotte, P. Zhai, M. Tignor, E. Poloczanska, K. Mintenbeck, A. Alegría, M. Nicolai, A. Okem, J. Petzold, B. Rama, N.M. Weyer (eds.)]. Cambridge University Press, Cambridge, UK and New York, NY, USA, pp. 321-445. 2019.

Osborne, M., Why we should be worried about the Mekong River's future: A perspective on forty years of great change. ISEAS Yusof Ishak Institute. http://hdl.handle.net/11540/11699. 2019.

Pawlowicz, R., Beardsley, B., Lentz, S.: Classical tidal harmonic analysis including error estimates in MATLAB using T_TIDE, Computers and Geosciences 28, 929-937, 2002.

Peng, D., Hill, E.M., Meltzner, A.J. and Switzer, A.D.: Tide gauge records show that the 18.61-year nodal tidal cycle can change high water levels by up to 30 cm, Journal of Geophysical Research: Oceans, 124(1), pp.736-749. 2019.

Pugh, D. and Woodworth, P.: Sea-level science: understanding tides, surges, tsunamis and mean sea-level changes, Cambridge University Press. 2014.

Rahman, M.M., Penny, G., Mondal, M.S., Zaman, M.H., Kryston, A., Salehin, M., Nahar, Q., Islam, M.S., Bolster, D., Tank, J.L. and Müller, M.F., Salinization in large river deltas: Drivers, impacts and socio-hydrological feedbacks. Water security, 6, p.100024. 2019.

Ritter, A. and Muñoz-Carpena, R. . Performance evaluation of hydrological models: Statistical significance for reducing subjectivity in goodness-of-fit assessments. Journal of Hydrology, 480, pp.33-45. 2013

Santiago-Collazo, F.L., Bilskie, M.V. and Hagen, S.C., A comprehensive review of compound inundation models in low-gradient coastal watersheds. Environmental Modelling & Software, 119, pp.166-181. 2019.

Sebastian, A., Bader, D.J., Nederhoff, C.M., Leijnse, T.W.B., Bricker, J.D. and Aarninkhof, S.G.J., Hindcast of pluvial, fluvial, and coastal flood damage in Houston, Texas during Hurricane Harvey (2017) using SFINCS. Natural hazards, 109, pp.2343-2362. 2021.

Seneviratne, S.I., N. Nicholls, D. Easterling, C.M. Goodess, S. Kanae, J. Kossin, Y. Luo, J. Marengo, K. McInnes, M. Rahimi, M. Reichstein, A. Sorteberg, C. Vera, and X. Zhang, 2012: Changes in climate extremes and their impacts on the natural physical environment. In: Managing the Risks of Extreme Events and Disasters to Advance Climate Change Adaptation [Field, C.B., V. Barros, T.F. Stocker, D. Qin, D.J. Dokken, K.L. Ebi, M.D. Mastrandrea, K.J. Mach, G.-K. Plattner, S.K. Allen, M. Tignor, and P.M. Midgley (eds.)]. A Special Report of Working Groups I and II of the Intergovernmental Panel on Climate Change (IPCC). Cambridge University Press, Cambridge, UK, and New York, NY, USA, pp. 109-230. 2012.

Seto, K.C., Exploring the dynamics of migration to mega-delta cities in Asia and Africa: Contemporary drivers and future scenarios. Global Environmental Change, 21, pp.S94-S107. 2011.

https://doi.org/10.5194/egusphere-2024-949
Preprint. Discussion started: 13 May 2024
© Author(s) 2024. CC BY 4.0 License.

Skliris, N., Marsh, R., Haigh, I., Wood, M., Hirschi, J.J., Darby, S., Quynh, N.P. and Hung, N.N., Drivers of rainfall trends in and around Mainland Southeast Asia. Frontiers in Climate. 2022.

Smajgl, A., Toan, T.Q., Nhan, D.K., Ward, J., Trung, N.H., Tri, L.Q., Tri, V.P.D. and Vu, P.T., Responding to rising sea levels in the Mekong Delta. *Nature Climate Change*, 5(2), pp.167-174. 2015.

Smith, G.P., Expert opinion: Stability of people, vehicles and buildings in flood water. https://doi.org/10.4225/53/58e1dfd63f1f4. 2015.

Syvitski, J.P. and Saito, Y., Morphodynamics of deltas under the influence of humans. Global and Planetary Change, 57(3-4), pp.261-282. 2007.

SwissRe: Industry-first Global Storm Surge Zones, https://www.swissre.com/dam/jcr:dedf399f-af17-4061-928f-dba8229c1499/industry_first_global_storm_surge_zones.pdf, Last access: 25 January 2021, 2017.

Takagi, H., Esteban, M. and Tam, T.T., Coastal vulnerabilities in a fast-growing Vietnamese City. In Coastal disasters and climate change in Vietnam (pp. 157-171). Elsevier. 2014.

Tessler, Z.D., Vörösmarty, C.J., Grossberg, M., Gladkova, I., Aizenman, H., Syvitski, J.P. and Foufoula-Georgiou, E., Profiling risk and sustainability in coastal deltas of the world. Science, 349(6248), pp.638-643. 2015.

Thanh VQ, Roelvink D, Van Der Wegen M, Reyns J, Kernkamp H, Van Vinh G, Linh VT. Flooding in the Mekong Delta: the impact of dyke systems on downstream hydrodynamics. Hydrology and Earth System Sciences. Jan 16;24(1):189-212. 2020.

Toan, T.Q., Climate change and sea level rise in the Mekong Delta: flood, tidal inundation, salinity intrusion, and irrigation adaptation methods. In Coastal disasters and climate change in Vietnam (pp. 199-218). Elsevier. 2014.

Tri, V.K., Hydrology and hydraulic infrastructure systems in the Mekong Delta, Vietnam. In The Mekong Delta System (pp. 49-81). F.G. Renaud and C. Kuenzer (eds.), The Mekong Delta System: Interdisciplinary Analyses of a River Delta, Springer Environmental Science and Engineering. Springer, Dordrecht. DOI 10.1007/978-94-007-3962-8_3. 2012.

Triet, N.V.K., Dung, N.V., Hoang, L.P., Le Duy, N., Tran, D.D., Anh, T.T., Kummu, M., Merz, B. and Apel, H., Future projections of flood dynamics in the Vietnamese Mekong Delta. Science of the Total Environment, 742, p.140596. 2020.

Try, S., Tanaka, S., Tanaka, K., Sayama, T., Khujanazarov, T. and Oeurng, C., Comparison of CMIP5 and CMIP6 GCM performance for flood projections in the Mekong River Basin. Journal of Hydrology: Regional Studies, 40, p.101035. 2022.

UNDRR. The human cost of disasters: An overview of the last 20 years (2000-2019). https://www.undrr.org/publication/human-cost-disasters-overview-last-20-years-2000-2019 . 2020

Valle-Levinson, A., Olabarrieta, M. and Heilman, L., Compound flooding in Houston-Galveston Bay during Hurricane Harvey. Science of the Total Environment, 747, p.141272. 2020.

Van, P.D.T., Popescu, I., Van Griensven, A., Solomatine, D.P., Trung, N.H. and Green, A., A study of the climate change impacts on fluvial flood propagation in the Vietnamese Mekong Delta. Hydrology and Earth System Sciences, 16(12), pp.4637-4649. 2012.

Västilä, K., Kummu, M., Sangmanee, C. and Chinvanno, S., Modelling climate change impacts on the flood pulse in the Lower Mekong floodplains. Journal of Water and Climate Change, 1(1), pp.67-86. 2010.

https://doi.org/10.5194/egusphere-2024-949
Preprint. Discussion started: 13 May 2024
© Author(s) 2024. CC BY 4.0 License.

Vousdoukas, M.I., Voukouvalas, E., Annunziato, A., Giardino, A. and Feyen, L.: Projections of extreme storm surge levels along Europe, Climate Dynamics, 47(9), pp.3171-3190. 2016.

Vasilopoulos, G., Quan, Q.L., Parsons, D.R., Darby, S.E., Tri, V.P.D., Hung, N.N., Haigh, I.D., Voepel, H.E., Nicholas, A.P. and Aalto, R., Establishing sustainable sediment budgets is critical for climate-resilient mega-deltas. Environmental Research Letters, 16(6), p.064089. 2021.

Wahl, T., Ward, P. J., Winsemius, H. C., AghaKouchak, A., Bender, J., Haigh, I. D., Jain, S., Leonard, M., Veldkamp, T. I. E., & Westra, S.. When environmental forces collide. EOS, 99. https://doi.org/10.1029/2018EO099745. 2018

Wahl, T., Jain, S., Bender, J., Meyers, S.D. and Luther, M.E., Increasing risk of compound flooding from storm surge and rainfall for major US cities. Nature Climate Change, 5(12), pp.1093-1097. 2015.

Wang, Q., Y. Xu, N. Wei, S. Wang, and H. Hu. Forecast and service performance on rapidly intensification process of Typhoons Rammasun (2014) and Hato (2017). Trop. Cyclone Res. Rev., 8, 18–26, https://doi.org/10.1016/j.tcrr.2019.07.002. 2019

Welch, A.C., Nicholls, R.J. and Lázár, A.N., Evolving deltas: Coevolution with engineered interventions. Elementa: Science of the Anthropocene, 5. 2017.

Wesselink A, Warner J, Syed MA, Chan F, Tran DD, Huq H, Huthoff F, Le Thuy N, Pinter N, Van Staveren M, Wester P. Trends in flood risk management in deltas around the world: Are we going 'soft'?: International Journal of Water Governance. Jan 1;3(4):25-46. 2015.

Williams, J., Horsburgh, K.J., Williams, J.A. and Proctor, R.N., Tide and skew surge independence: New insights for flood risk. Geophysical Research Letters, 43(12), pp.6410-6417. 2016.

Ward, P.J., Couasnon, A., Eilander, D., Haigh, I.D., Hendry, A., Muis, S., Veldkamp, T.I., Winsemius, H.C. and Wahl, T., Dependence between high sea-level and high river discharge increases flood hazard in global deltas and estuaries. Environmental Research Letters, 13(8), p.084012. 2018.

Wood, M., Haigh, I.D., Le, Q.Q., Nguyen, H.N., Tran, H.B., Darby, S.E., Marsh, R., Skliris, N., Hirschi, J.J.M., Nicholls, R.J. and Bloemendaal, N., Climate-induced storminess forces major increases in future storm surge hazard in the South China Sea region. Natural Hazards and Earth System Sciences Discussions, pp.1-32. 2023.

Yamazaki, D., de Almeida, G.A. and Bates, P.D., Improving computational efficiency in global river models by implementing the local inertial flow equation and a vector-based river network map. Water Resources Research, 49(11), pp.7221-7235. 2013.

Yamazaki, D., Kanae, S., Kim, H. and Oki, T., A physically based description of floodplain inundation dynamics in a global river routing model. Water Resources Research, 47(4). 2011.

Yue, S., Ouarda, T.B., Bobée, B., Legendre, P. and Bruneau, P., Approach for describing statistical properties of flood hydrograph. Journal of hydrologic engineering, 7(2), pp.147-153. 2002.

Zscheischler, J., Westra, S., Van Den Hurk, B.J.J.M., Seneviratne, S.I., Ward, P.J., Pitman, A., AghaKouchak, A., Bresch, D.N., Leonard, M., Wahl, T. and Zhang, X., Future climate risk from compound events. Nat Clim Change 8: 469–477. 2018.